



Powerful **A**dvanced **N**-Level **D**igital **A**rchitecture
for models of electrified vehicles and their components

Research Innovation Action

GA # 824256

EUROPEAN COMMISSION
Horizon 2020 | GV-02-2018

Virtual product development and production of
all types of electrified vehicles and components

Deliverable No.	PANDA D2.1	
Deliverable Title	Multi-level knowledge models of batteries	
Deliverable Date	2019-11-30	
Deliverable Type	REPORT	
Dissemination level	Public (PU)	
Written By	Joris JAGUEMONT (VUB), Calin HUSAR (SISW), Ronan GERMAN (ULille)	2019-10-10
Reviewed by	Wim VAN der KUYLEN (Blueway). Ronan GERMAN (ULille) – except section 6 -	2019-11-09 2019-11-09
Approved by	Alain BOUSCAYROL (ULille) - Coordinator	2019-11-22
Status	Final	2019-11-22

Publishable Executive Summary

Leader: Dr. Joris JAGUEMONT (VUB), Participants: ULille, TUV, SISW, and Bluways

The objective of the project PANDA is to provide a disruptive and open access model organization for an easy interconnection and change of models in the development process of EVs. This report is dedicated to the development of multi-scale multi-domain models of batteries (from individual cells to battery packs) for real-time simulation and on-line diagnostics. Multi-scale multi-domain models will, therefore, be developed for the battery subsystem and organized with the unified methodology developed in WP1.

In order to develop the knowledge model, a first characterisation campaign is proposed to capture the electrical and thermal behavior of the selected cell technology (NMC). Then, with the parameters acquired in the characterisation phase, the development of the NMC-based semi-empirical model is proposed at the cell level and battery pack level using Matlab / Simscape environment. Real driving profile monitored from the Zoe Renault vehicle is used for the validation of the model.

Additionally, the adaptation and validation of the models to Simcenter Amesim using the new Energetic Macroscopic representation (EMR) based library are ensured by SISW. A good agreement is found between the experimental values and the simulation results. Finally, the Report closes with discussion and conclusion.

Contributions:

<i>No</i>	<i>Who</i>	<i>Description</i>	<i>Date</i>
1	VUB	D2.1 report creation and outline	2019-07-01
2	VUB	Section 1, 2 and 3	2019-08-01
3	VUB	Section 4	2019-09-01
4	VUB	Section 5	2019-10-01
5	ULille	Section 6	2019-10-01
6	SISW	Section 7	2019-11-01
7	VUB	Update and conclusion	2019-11-27

Contents

1.	Introduction.....	6
2.	Development of test methodology for characterization of batteries	6
2.1.	Cell selection process	6
2.2.	Cell datasheet	7
2.3.	Characterization protocol.....	8
2.4.	Electrical characterization	9
2.4.1.	Discharge capacity test	9
2.4.2.	OCV vs SoC test procedure	9
2.4.3.	HPPC test procedure	10
2.4.4.	Validation tests	11
2.5.	Thermal characterization.....	13
2.5.1.	Temperature measurement.....	13
2.5.2.	Thermal heat capacity test	13
2.5.3.	Validation tests	14
3.	Electro-thermal characterization results of the NMC cell.....	15
3.1.	Results from standard data collection for electrical modelling.....	15
3.1.1.	Results from the discharge capacity test	15
3.1.2.	Results from the OCV test.....	15
3.1.3.	Results from the HPPC test	16
3.1.4.	Results from the electrical validation tests.....	18
3.2.	Results from standard data collection for thermal modelling.....	19
3.2.1.	Temperature measurement.....	19
3.2.2.	Thermal validation tests	19
3.3.	Conclusion on the characterisation	20
4.	Electro-thermal modelling results of the NMC cell	21
4.1.	Description of the used methodology	21
4.2.	Development of the electrical model	21
4.2.1.	Description of the electrical model.....	21
4.2.2.	Results of the characterization for electrical modelling	22
4.2.3.	Results of the validation for electrical modelling	25
4.3.	Development of the 1D-thermal model	28
4.3.1.	Description of the 1D-thermal model.....	28
4.3.2.	Results of the characterization for thermal modelling	29
4.3.3.	Results of the validation for thermal modelling	30
4.4.	Conclusion on the 1D-electro-thermal modelling	30
5.	Development of the NMC battery pack model in Matlab / Simulink	32
5.1.	The structure design of the PANDA P-HEV battery pack	32
5.2.	Battery pack model methodologies.....	32
5.3.	1D-electro-thermal model development of the pack.....	33
5.4.	Validation results.....	34
6.	Development of the NMC battery pack model in Matlab using EMR	36
6.1.	Validation results.....	36
6.2.	EMR representation of the battery pack model.....	37
6.2.1.	Reorganization of the Simulink electro-thermal model for the single-cell.....	37
6.2.2.	EMR of the electro-thermal model for one cell	38
6.2.3.	Comparison of the two representations (block diagrams and EMR).....	38
7.	Development of the NMC battery pack model in Simcenter Amesim using EMR	40
7.1.	Simcenter Amesim Electric Storage (ESS) library.....	40
7.1.1.	Library content.....	40
7.1.2.	Cell and pack models	41
7.1.3.	Notations and conventions.....	42
7.2.	EMR-based battery model in Simcenter Amesim	43
8.	Conclusions.....	47
9.	Deviations.....	47
10.	References	47

11. Acknowledgments.....	49
Appendix A – EMR graphical pictogram.....	50
Appendix B – Modelling approach of batteries in Simcenter Amesim	51
B1.1 Parameter setting tools.....	51
B1.2 Pre-calibrated Tool.....	51
B1.3 Battery Pre-Sizing Tool	52
B1.4 Battery Datasheet Import Tool	52
B1.5 Battery Identification Assistant	53
B1.6 Transform into RC	53
B1.7 BDS Import Tool	53
B1.8 Simcenter Amesim model validation	54
Appendix C – Quality Assurance	58

Figures

Figure 1: NMC Kokam pouch cell 40Ah.....	7
Figure 2. Example of an HPPC pulse train	10
Figure 3. Example of a WLTC driving profile	12
Figure 4. WLTC profile with repetition for a sample cell at 25 degrees.....	12
Figure 5. Micro-pulse test at 25°C.....	13
Figure 6. Discharge capacity tests at different temperatures at C/5	15
Figure 7. Discharge OCV test profile for the NMC cell at 25°C.....	16
Figure 8: OCV curves of the NMC cell at different temperatures with discharge OCV curve (top) and charge OCV curve (bottom)	16
Figure 9. On the left: HPPC pulse train at 25°C with the current profile and voltage output response. On the right: example of a pulse train (closer loop).....	17
Figure 10. Internal resistance evolution at different temperatures for a discharging (top) and charging (bottom) state at C/5.....	18
Figure 11. WLTC profile as a function of temperature.....	18
Figure 12. Temperature point for the NMC Kokam cell at different time intervals.....	19
Figure 13. Temperature variation at 2C for a constant discharge test.	20
Figure 14. Schematic of the modelling methodology	21
Figure 15: representation of the 1st-order Thevenin model	22
Figure 16. Left: HPPC pulses at certain SoC, Right: Corresponding region of the Thevenin ECM to the current pulses.	22
Figure 17. Discharge (top) and charge (bottom) OCV as a function of temperature and state of charge.	23
Figure 18. Ohmic resistance as a function of temperature and state of charge for the discharging (top) and charging states (bottom).....	24
Figure 19. Polarization resistance as a function of temperature and state of charge for the discharging (top) and charging states (bottom).....	24
Figure 20. Equivalent capacitance as a function of the current rate and state of charge for the discharging (top) and charging states (bottom).....	25
Figure 21. Validation of the NMC electrical model at 25°C.....	26
Figure 22. Validation of the NMC electrical model at 45°C.....	26
Figure 23. Validation of the NMC electrical model at 10°C.....	27
Figure 24: Overview of the thermal model with a thermal modelling schematic for the NMC Kokam cell.	28
Figure 25. Example of the fitting curve exercise at 25°C where the fitted temperature curve has been created using Equation (7).	29
Figure 26. NMC specific heat capacities at different temperatures and at 50% of SOC.	30
Figure 27. Validation of the NMC thermal model at different initial temperatures.	30
Figure 28. The structure design of the 360V Zoe battery pack with 12 modules.	32
Figure 29. Matlab / Simulink model of the battery pack system.	34
Figure 30. Validation of the NMC electrical model at 25°C.....	35
Figure 31. Validation of the NMC thermal model at different initial temperatures.	35
Figure 32. Electro-thermal coupling principle.....	36
Figure 33. The power exchange between pictograms.	37
Figure 34. EMR of the dynamical electro-thermal model for a single cell.	38
Figure 35. Evolution of the input current.....	39

Figure 36. Evolution of the cell voltage.....	39
Figure 37. Evolution of the cell temperature.....	39
Figure 38. Electric Storage library display.....	40
Figure 39. Electric Storage subfolder icon content.....	40
Figure 40. Batteries subfolder icon content.....	41
Figure 41. Cell and pack electrical connection.....	41
Figure 42. Battery cell icon examples.....	41
Figure 43.: Battery pack icon examples.....	41
Figure 44. Battery pack and battery cell comparison model.....	42
Figure 45. ESS dipoles use the passive convention.....	42
Figure 46. The passive convention is indicated with a white dot on the icons.....	42
Figure 47. Equivalent circuit models: ideal voltage source model (left), NMC model (right).....	43
Figure 48. EMR energy source element.....	43
Figure 49. EMR of the BEV.....	43
Figure 50. EMR of the NMC battery model.....	44
Figure 51. Battery interconnection variables.....	44
Figure 52. Graph of the battery power.....	44
Figure 53. Armature current.....	45
Figure 54. Vehicle velocity.....	45
Figure 55. Armature windings current control system.....	46
Figure 56. EMR diagram focus on the current control loop.....	46
Figure 57. The workflow of the Pre-calibrated Tool.....	52
Figure 58. Battery Pre-Sizing Tool objectives.....	52
Figure 59. Battery Datasheet Import Tool objectives.....	53
Figure 60. Battery Assistant objectives.....	53
Figure 61. The workflow of the BDS Import Tool.....	54
Figure 62. Imported model of the BDS Import Tool.....	54
Figure 63. Current profile used for HEV road operation validation.....	55
Figure 64. Quasi-static circuit model.....	55
Figure 65. Sketch of the pre-calibrated NMC-C HP model.....	55
Figure 66. Comparison between experimental voltage and modeling voltages during a typical HEV and EV duty cycles current.....	56
Figure 67. Detailed view of voltage during typical HEV duty cycle.....	57

Tables

Table 1. NMC 40Ah Kokam cell characteristics.....	7
Table 2. Overview of the defined tests in the standard ISO/CD 12405 ½ and IEC 62660-1.....	8
Table 3. Discharge capacity test procedure.....	9
Table 4. OCV vs SOC test procedure.....	10
Table 5. HPPC test procedure.....	11
Table 6. Electrical validation test procedure.....	12
Table 7. The thermal validation test procedure.....	14
Table 8. Capacity values for different temperatures.....	15
Table 9. Electrical model deviation.....	27
Table 10: Dependence of the model parameters.....	36
Table 11: EMR variables for electro-thermal modelling.....	37
Table 12: Project Partners.....	49
Table 13: EMR pictogram.....	50
Table 14. Overview of the battery models.....	51

1. Introduction

The project PANDA provides a disruptive and open access model organization for an easy interconnection and change of models in the development process of EVs. To achieve this goal, in WP2, a multi-scale multi-domain model of batteries according to the PANDA methodology will be provided as well as a “cloud real testing” of batteries will be achieved as a demonstration. In this report, the development of the multi-level knowledge model is described.

First, the selected cell technology for the WP2 will be introduced. Then, a dedicated test methodology will be developed to reflect the battery behaviour as close to reality. It will be based on different developed techniques:

- The experiences from the standardization organizations regarding batteries such as IEC, ISO, SAE, JAR
- Measured real load profiles of batteries from electric vehicles heavy-duty vehicles, covered in WP2
- Characterization techniques such as advanced pulse testing, recently optimized for batteries at VUB.

Additionally, a needed in-depth cell characterization will be conducted. It will provide a detailed understanding of the short- and medium-term behaviour of the battery cells. This characterization will take into account the electric and thermal aspects of the cells as well as a statistical spread on battery cell behaviour for the development process of the electrical and thermal models. The electrical and thermal behaviour of the battery cells will be investigated at different and well-selected operating conditions: in particular at different temperature levels, with different current rates and at different values of the state of charge. The models will be validated according to the requirement of WP5.

Moreover, the third task will consist in developing a dynamic electric-thermal battery model able to predict, accurately the electrical and thermal responses and behaviours of the battery cell under a wide range of stress conditions. The model will be developed in Matlab / Simulink environment. The task will be extended to a battery pack system for which testing, simulation and validation will be proposed.

Finally, the developed modelling method will be integrated into an industrial software package known as Simcenter AMESim, a well know structural software in the automotive industry. The challenge will be to develop a similar battery pack model as the one in Matlab using a dedicated functional causal library based on the WP1 approach using EMR (Energetic Macroscopic Representation).

2. Development of test methodology for characterization of batteries

2.1. Cell selection process

The goal of WP2 is to provide different multi-scale multi-domain models of batteries according to the WP1 unified method. A battery Cloud-Computing real testing will also be achieved as a demonstration.

The modelling methodologies will be applied to existing vehicles and virtual testing will be validated based on the measurement of these real vehicles. Moreover, an innovative concept of Plug-in HEV (P-HEV) will also be considered with virtual and real testing of its electrical subsystems. In order to check the interest of the proposed methods, different cases will be studied.

- 1) A BEV (Battery Electrical Vehicle), provided by Renault Technologie Roumanie (RTR), a Renault Zoe which parameter are available and with an instrumented vehicle and 32 km of different road profiles for driving tests. The virtual testing will be compared with the previous development.
- 2) A light Fuel Cell Vehicle (FCV) from the FP7 MobyPost project, provided by UBFC. All parameters and Fuel Cell test bench are available, as well as some driving tests. The virtual testing will be compared with the previous development.
- 3) An innovative Plug-in Hybrid Electric Vehicle (P-HEV), based on a demo car of Valeo (VEEM). A series-parallel HEV with a 48V battery and low-voltage electrical machines will be considered. The new electrical subsystems (batteries and e-drive) will be studied both in virtual and real testing.

The cell pre-selection process consists of selecting a cell technology that is both available and meets the requirements of the three applications. Among all candidates, the mentioned NMC cell (Kokam 40 Ah), presented in Figure 1, meets all specifications of the three applications. Therefore, the WP2 methodology and characterization will be focused on this selected cell.



Figure 1: NMC Kokam pouch cell 40Ah

2.2. Cell datasheet

In order to reflect the battery behaviour as close to reality, a dedicated test methodology is developed based on the NMC 40Ah Kokam cell. The characteristic of the prismatic NMC-based cell is reported in Table 1.

Table 1. NMC 40Ah Kokam cell characteristics.

		NMC 40Ah
	Material	
Chemistry		NMC
Shape		Pouch
	Voltage	
Nom. Voltage (V)		3.6
End of charging voltage (EOCV V)		4.15
End of discharging voltage (EOD V)		3.0
	Energy	
Capacity (Ah)		40
Specific Energy (nominal - Wh/kg)		160
Energy Density (nominal - Wh/L)		338
	Current DCH	
Continuous rms DCH (A)		80A – 2C
max DCH pulse 10s (A)		80A – 2C
	Current CHA	
Continuous rms CHA (A)		80A – 2C
max CHA pulse 10s (A)		
max CHA pulse 60s (A)		
Fast charge max 360s (A)		120A – 3C
	Mechanical	
Weight (kg)		0.920
Volume (L)		0.49
Dimensions LxWxH (mm)		225x224x9.8
	Cost	
Price per piece (€/ piece)		/

2.3. Characterization protocol

One of the main objectives of this test methodology is to secure the development process of the electrical and thermal models in Task 2.1. The development process of battery modelling consists of a series of standard testing procedures used for many years in the automotive industry in order to capture efficiently the electrical and thermal behaviours. Table 2 gives an overview of the available standard testing procedures for specific tests for reviewing the characteristics and performance parameters of lithium-ion batteries for BEV and for HEV applications.

Table 2. Overview of the defined tests in the standard ISO/CD 12405 ½ and IEC 62660-1.

Test item	Test	Condition	Pack/System ISO/CD 12405-1/2	Extended	Cell IEC 62660-1	Extended
Pre-conditioning	Cycling	Temperature	25 °C		25 °C	
		Charge	standard charge		Standard Charge	
		Discharge	2C		0.2C	2I _r
		# Cycles	5		5	
Energy and capacity	CC discharge	Temperature	-18 °C, 0 °C, 25 °C, 40 °C		-20 °C, 0 °C, 25 °C, 45 °C	
		Charge	standard charge	# I _r -rates until max charge I _r -rate (as 1/3I _r , 1I _r , 2I _r , ...)	standard charge	# I _r -rates until max charge I _r -rate (as 1/3I _r , 1I _r , 2I _r , ...)
		Discharge	1C, 10C, 20C, I _{max}	1/3I _r , 2I _r , 5I _r	1C, 10C, 20C, I _{max}	1/3I _r , 2I _r , 5I _r
		# cycles	2		2	
Power and resistance	Pulse charge/discharge	Temperature	-18 °C, 0 °C, 25 °C, 40 °C		-20 °C, 0 °C, 25 °C, 45 °C	40 °C instead of 45 °C
		Discharge	I _{max, dis}	1/3I _r , 2I _r , 5I _r , 10I _r	0.2C, 1C, 5C, 10C	1/3I _r , 2I _r , I _{max}
		Duration	0.1 s, 2 s, 10 s, 18 s		10 s	
		Charge	0.75*I _{max, dis}	1/3I _r , 2I _r , 5I _r , 10I _r , I _{max}	1/3C, 1C, 5C, 10C	2I _r , I _{max}
		Duration	0.1 s, 2 s, 10 s		10s	
		SoC	80%, 65%, 50%, 35%, 20%		50%	80%, 65%, 35%, 20%
Energy efficiency	Pulse charge/discharge	Temperature	0 °C, 25 °C, 40 °C	-18 °C	-20 °C, 0 °C, 25 °C, 45 °C	40 °C instead of 45 °C
		Discharge	See sequence in Table 4	1/3I _r , 1I _r , 2I _r , 5I _r , 10I _r , I _{max}	1/3C, 1C, 5C, 10C	2I _r , I _{max}
		Duration		10s	10s	
		Charge	See sequence in Table 4	1/3I _r , 1I _r , 2I _r , 5I _r , 10I _r , I _{max}	1/3C, 1C, 5C, 10C	2I _r , I _{max}
		Duration		10 s	10 s	
		SoC	65%, 50%, 35%	80%, 20%	50%	80%, 65%, 35%, 20%

2.4. Electrical characterization

The electrical characterization of the cells is performed by implementing a characterization testing scheme derived from Table 2 and composed of the following subsequent characterization tests:

- Discharge capacity test
- HPPC test
- OCV test
- Validation test

Almost all of the tests will be conducted at different temperatures in order to have a wide range of mobility for the model. The testing temperatures are selected in order to have different conditions and to represent the cell in extreme environmental conditions. A set of 6 cells will be characterized for accuracy, performing different tests at:

- 10°C for the low-temperature environment
- 25°C for ambient temperature environment
- 45°C for high-temperature environment

The next sub-sections are dedicated to the description of each of these listed tests.

2.4.1. Discharge capacity test

The objective of this test is fairly straightforward. The discharged cell capacity expressed in Ah at different discharge C-rates (or I_t) and temperatures are obtained from the test results. Basically, it consists of performing full charges and discharges at different C-rates to obtain stable capacity measurements. This test is an important step as this capacity value is the reference value used for the other tests composing the characterization testing procedures. In addition, the C-rates chosen in this test are also used in the next tests. The “Discharge Capacity test” is conceptually described below:

Table 3. Discharge capacity test procedure.

Capacity Test			
Step	Action	C-Rate	Limit
		NMC	
1	Tempering	T = 10°C, 25°C and 45°C	3h
2	Standard charge	C/2	> EOCV < 0.05 C-Rate
3	Pause		30 min
4	Discharge	C/2	EODV
5	Pause		30 min
6	Standard charge	C/5	> EOCV < 0.05 C-Rate
7	Pause		30 min
8	Discharge	C/5	EODV
9	Pause		30 min

2.4.2. OCV vs SoC test procedure

In order to determine the relationship between the open-circuit voltage (OCV) and the state of charge (SoC) of the battery, the OCV-test is performed according to the description given here below.

The test profile consists of a complete charge following by complete discharge of the cell in steps of 5% between 100% and 0% SoC window of the available discharge capacity of the battery at C/5 (8A). The capacity related to this C-rate will be already available from the calculation during the “Discharge Capacity Test” at the C/5 discharge pulse for each temperature. After each step, a relaxation period of 3h has been implemented, as it can appear long but necessary rest time for relaxation. The OCV value at that specific SoC levels is then defined as the voltage

at the end of the 3h-relaxation period. Then, the battery is completely discharged and a series of charge pulses are applied in order to have the discharging and charging OCV behaviours. The voltages during each rest period are recorded to establish the cell's OCV behaviour. From these data, OCV against SOC values can be estimated by straight-line interpolation or by curve fitting through the measured data points. Based on the obtained OCV values, a look-up table can be generated for the prediction of the OCV in the function of the battery SoC for future battery models.

Table 4. OCV vs SOC test procedure.

Step	Action	OCV vs SOC	
		C-Rate	Limit
		NMC	
1	Tempering	T = 10°C, 25°C and 45°C	3h
2	Standard charge	C/5	> EOCV <0.05C-Rate
3	Pause	3 hours	
4	Discharge	C/5	Δ DOD = 5%
5	Pause	3 hours	
6	Charge	C/5	Δ DOD = 5%
7	Pause	3 hours	

2.4.3. HPPC test procedure

The hybrid pulse power characterization (HPPC) test is intended to measure the battery impedance using a test profile that incorporates both discharge and charge pulses, as shown in Figure 2. The primary objective of this test is to establish the DC internal resistance of the three tested cells. The internal resistance is responsible for the irreversible heat generation and a measurable degradation is expected that increases its value at every SoC and C-rate. Hence, as a function of the SoC, of the current rate, and of the temperature, the internal DC resistance is determined on a large range of SoC points, currents, and temperatures.

The idea of this test is to apply a 10-second discharge-pulse and 10-second charge-pulse power capabilities at each given SoC and for different C-rates. A 600s-rest period is scheduled between each HPPC pulse. From the result data, an algorithm will afterwards determine the DC internal resistance of the cell.

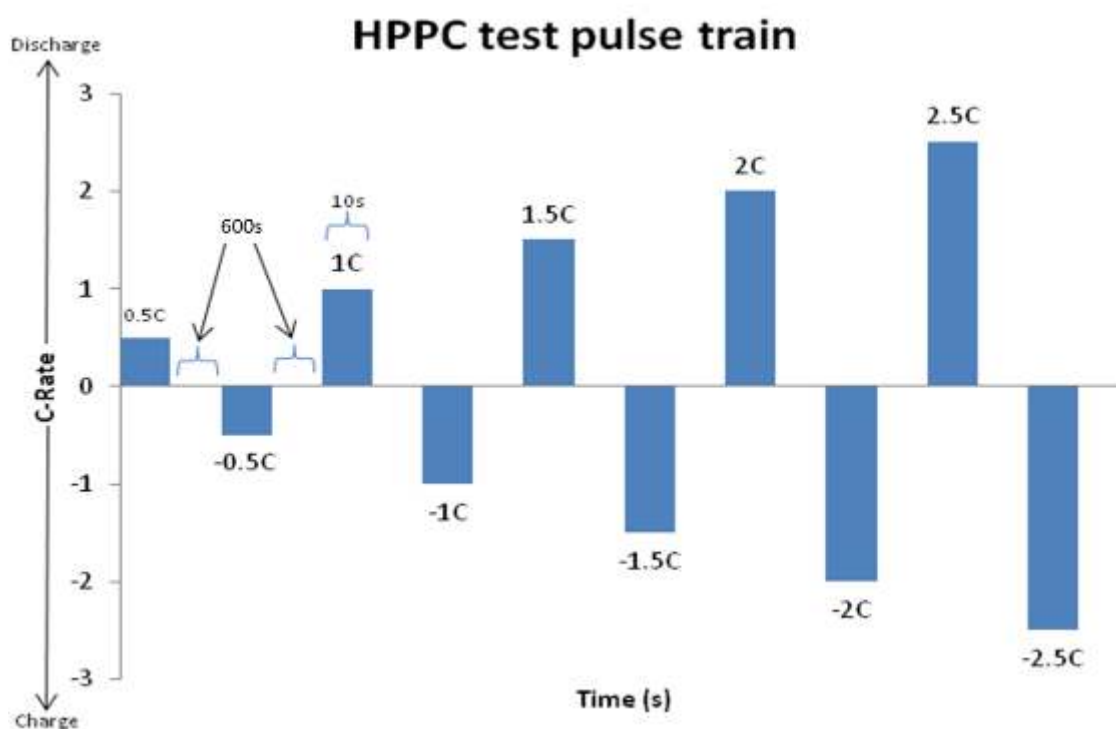


Figure 2. Example of an HPPC pulse train

The HPPC test procedure is conceptually described in the table below:

Table 5. HPPC test procedure.

HPPC Test			
Step	Action	C-Rate	Limit
NMC			
1	Tempering	T = 10°C, 25°C and 45°C	3h
2	Standard charge	1C	> EOCV
3	Pause		<0.05 C-Rate
4	Discharge	1C	3 h
5	Pause		Δ DOD = 5%
6			3 h
NMC			
Acc T (s)			
10 C/5			
610 PAUSE			
620 - C/5			
1220 PAUSE			
1230 C/3			
1830 PAUSE			
1840 - C/3			
2440 PAUSE			
2450 C/2			
3050 PAUSE			
3060 - C/2			
3660 PAUSE			
3670 1C			
4270 PAUSE			
4280 - 1C			
4880 PAUSE			
4890 1.5C			
5490 PAUSE			
5500 - 1.5C			
6100 PAUSE			
6110 2C			
6710 PAUSE			
6720 - 2C			
7320 PAUSE			
Repeat steps 3 - 6 until DoD 90%			

2.4.4. Validation tests

In order to correctly validate the electrical models created based on the parameters acquired from the different characterization tests, some independent validation tests are additionally performed. These tests can be used to compare the output of the model with the voltage response of the cell.

The worldwide harmonized light vehicles (WLTC) test procedure has been selected in order to perform the validation of the electrical model. During the 1990s, the emergence of electric road vehicles powered by alkaline batteries pushed the development of suitable test procedures and standards. Conventional constant current discharge tests were defined for lead-acid batteries, but they did not reflect the actual use pattern of the batteries in electric vehicles. The WLTC test procedure used for electrical validation is based on the WLTC driving cycle that was developed in collaboration of the EU, Japan, and India under the guideline of UNECE World Forum for Harmonization of Vehicle Regulations. In the framework of PANDA and Task 2.1, a current load profile representing a high-power application has been derived based on the WLTC driving profile as shown by Figure 3.

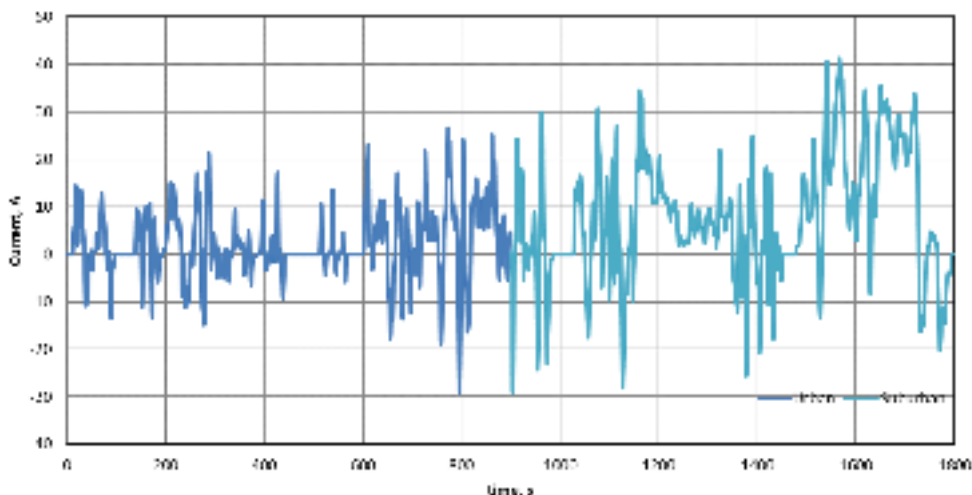


Figure 3. Example of a WLTC driving profile

The WLTC validation consists of standard charge procedure followed by the continuous repetition of WLTC current load profile as shown by the example in Figure 4.

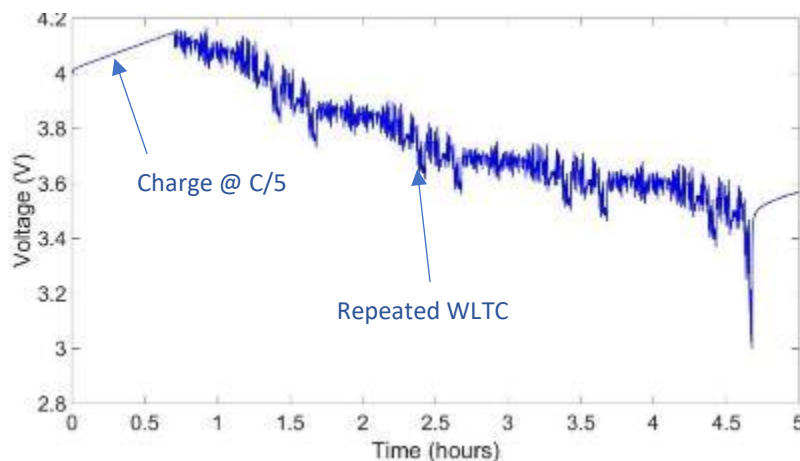


Figure 4. WLTC profile with repetition for a sample cell at 25 degrees

Table 6. Electrical validation test procedure.

Electrical validation Test			
Step	Action	C-Rate	Limit
1	Tempering	NMC T = 10°C, 25°C and 45°C	3h
2	Standard charge	C/5	> EOCV < 0.05 C-Rate
3	Pause		30 min
4	DCH	C/5	Δ DOD = 5% to 90%SoC
5	Pause		30 min
6	Cycle	WLTC	From 90%SoC to 10%SoC
7	Pause		30 min

Steps 2-7 are repeated three times for each T

2.5. Thermal characterization

The thermal characterization of the cells is performed by implementing a characterization testing scheme derived from Table 2 and composed of the following subsequent characterization tests:

- thermal heat capacity test,
- validation test.

The next sub-sections are dedicated to the description of each of these listed tests.

2.5.1. Temperature measurement

For every test, a maximal allowable temperature is defined to prevent gassing and critical failure of the cell resulting from overheating and thermal runaway. Also, the evolution of the temperature is an important parameter for designing a thermal model. Thus, it is necessary to have a reliable way of measuring battery temperature.

Because with the test equipment available only one physical point of the battery can be measured for temperature, this point has to be carefully chosen. To select the right temperature point, IR images of the cell will be captured by a Ti25 thermal imager (FLUKE®, Everett, WA, USA) at regular time intervals during a high-current discharge capacity test (2C or 80A). The IR thermography will show the highest temperature point of the cell for which the thermocouple will be placed.

2.5.2. Thermal heat capacity test

One usual manner to determine the C_p is to use calorimetry. However, such equipment is quite expensive especially when the tested cell presents quite a volume like for prismatic-shape cells. In this project, we propose a method to assess this parameter without the use of any calorimeter. The method used to assess the specific heat capacity involves high current rate in order to reach the thermal steady state of the system for which the generated heat is equal to heat losses by the system.

As shown in Figure 5, the profile used in this report to assess the specific heat capacity (C_p) involves charging and discharging pulses at the manufacturer's recommended maximum rates. The profile is called a micro-pulse and is conducted around a fixed SOC of 50%. The first goal of this profile is to extract and inject the same number of Ah to the cell, in order to not have a dependency of the SOC, which can influence electrical and thermal parameters such as the cell resistances. The second aim to this profile is to reach a steady temperature at which the cell starts to lose the same amount of heat it is gaining (steady-state), where thermal parameters such as convective heat transfer can be obtained. As for the C_p , the period, for which the surface temperature is increasing (transient state), is considered for comparison with the model. Then, the test profile is repeated at different temperatures to obtain the parameters' behaviour with temperature.

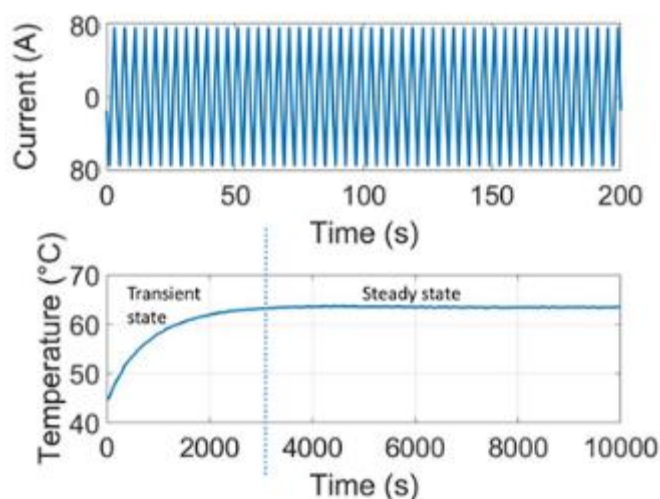


Figure 5. Micro-pulse test at 25°C

The heat capacity test consists of performing different external heating tests in order to evaluate the temperature increase of the cells when no heat is lost to the surrounding area. All the supplied heat is ideally

accumulated in the cell's body. By knowing the mass of the cells and the voltage and current supplied to the heater, the specific heat capacity value can be calculated at any temperature or over any temperature range as:

$$C_p = \frac{Q}{m\Delta T} \quad (1)$$

where C_p is the specific heat capacity (kJ/kg.K), Q the heat generation rate (W), m the mass of the cell (m) and ΔT the temperature difference.

2.5.3. Validation tests

In order to correctly validate the thermal models created based on the parameters acquired from the different characterization tests, two independent types of validation tests are additionally performed: the constant current and dynamic current test. These tests can be used to compare the output of the model with the temperature response of the cell.

The constant current validation test consists of discharging and charging profiles at high C-rates and 100% SOC levels will be performed. To ensure the maximal heat generation, a discharging current of 2C (80A) is applied.

Table 7. The thermal validation test procedure.

Step	Action	Thermal validation test	
		C-Rate	Limit
		NMC	
1	Tempering	T = 10°C, 25°C and 45°C	3h
2	Standard charge	0.5C	> EOCV <0.05 C-Rate
3	Pause		30 min
4	DCH	2C	to 0%SoC
5	Pause		30 min

3. Electro-thermal characterization results of the NMC cell

3.1. Results from standard data collection for electrical modelling

A set of 6 cells has been characterized by performing different tests described in the section earlier. In this section, the electrical and thermal results are presented.

3.1.1. Results from the discharge capacity test

As mentioned in the overview the cells at different temperatures were charged at a 0.2C / 0.5C rate and then discharged at 0.2C / 0.5C respectively. The results for one of the cells at various temperatures is shown in Figure 6, below. Table 8 reports the discharge capacity of the NMC-based cell at different temperatures and different low C-rates. A general increasing trend of the capacities can be observed with increasing temperatures which could be explained by kinetics at higher temperatures. Moreover, the capacity values are lower when the C-rate is increasing which is in accordance with the Peukert's Law [Omar 2013]. However, at low temperatures, the capacity values are lower with a decreasing C-rate, this is due to the sluggish electrochemical reaction resulting from the low-temperature which is blocking the cell capacity. This justifies why at higher C-rates, due to the produced heat from self-heating [Jaguemont 2015], [Jaguemont 2016], the capacity values are higher. In addition, the values obtained by the experiment are very close to the manufacturer quoted data which shows the solid accuracy of the data displayed in this report.

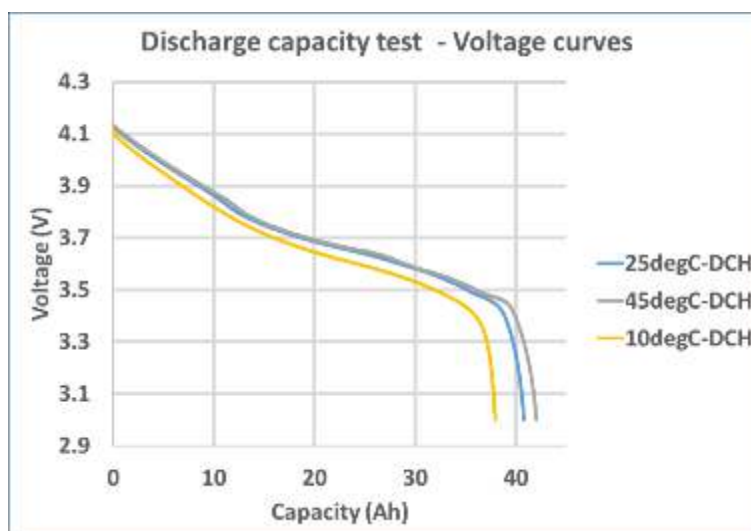


Figure 6. Discharge capacity tests at different temperatures at C/5

Table 8. Capacity values for different temperatures.

C-rate	C/5 (0.2C)		
Temperature	10°C	25°C	45°C
Discharge capacity (Ah)	38	41	42
C-rate	C/2 (0.5C)		
Temperature	10°C	25°C	45°C
Discharge capacity (Ah)	36	40	41

3.1.2. Results from the OCV test

Another important electrical characterization test is the OCV test. This test provides the open-circuit voltage of the cell at different levels of the state-of-charge (SOC). The OCV curve was determined for both the charge and the discharge condition of the NMC-based cell and was determined at different values of the temperature.

OCV characterization for 25°C is shown in Figure 7 and OCV curves for all test is shown in Figure 8. It can be seen that the values at low and high SoC in the OCV characterization reflect clearly the non-linear voltage evolution. The values can be used for the electrical model for the battery voltage equation. Moreover, based on the

obtained OCV values, a look-up table can be generated for the prediction of the OCV in the function of the battery SOC for the electrical modelling part.

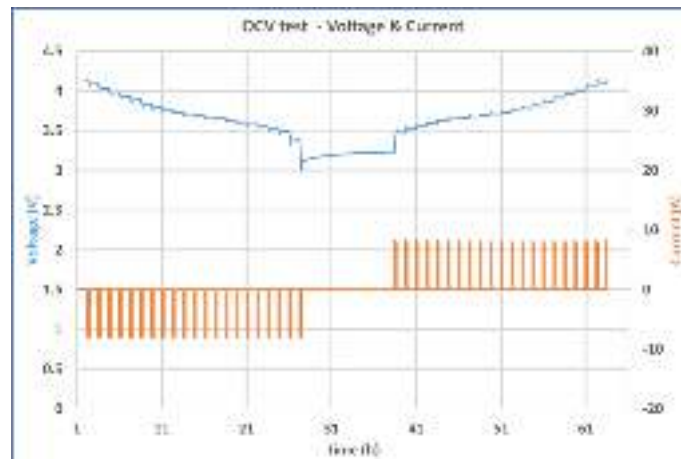


Figure 7. Discharge OCV test profile for the NMC cell at 25°C

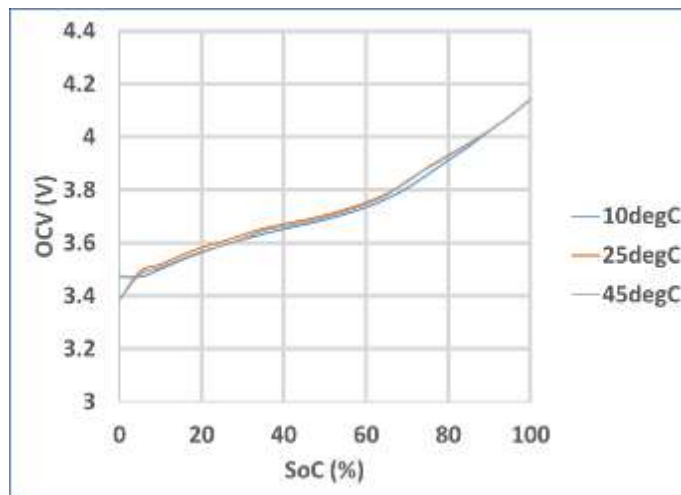
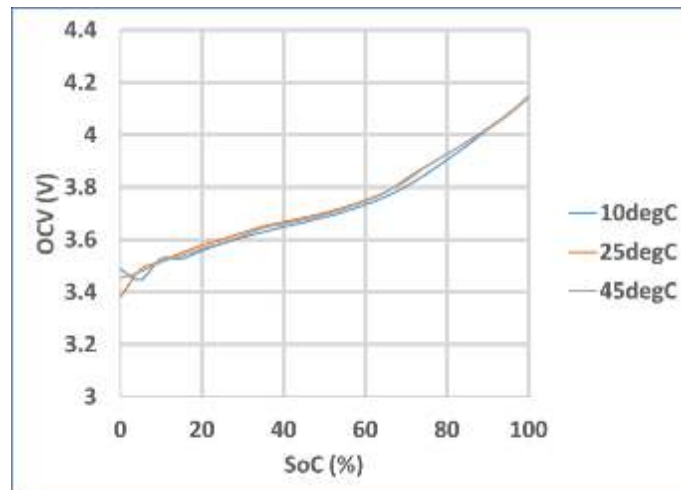


Figure 8: OCV curves of the NMC cell at different temperatures with discharge OCV curve (top) and charge OCV curve (bottom)

3.1.3. Results from the HPPC test

The HPPC test is intended to measure the battery impedance using a test profile that incorporates both discharge and regen pulses. The primary objective of this test is to establish, as a function of SOC, the internal resistance of the tested cell. A representative figure showing the current pulses implemented is shown in Figure 9. During

the 10-sec charge and discharge pulses, extended voltage limits have been used: A preliminary simulation can be performed taking as validation profile the different pulses performed information to the model to simulate the behaviour of the studied lithium-ion cells and to extract the electrical parameters needed for the model (R_0 , R_1 , and C_1). The methodology for the extraction is explained in the next section.

The HPPC characterization result is shown in Figure 10, with the values of the discharge and charge internal resistance at C/5. As shown in this figure, the internal resistance is higher at lower SoC levels and decreases with increase in SoC level. Moreover, regarding the temperature influence, the resistance values appear to be similar at a higher temperature and for both states. On the other hand, the resistance seems higher for both states at lower temperatures. This is due to sluggish electrochemical reactions and higher electrolyte frictions occurring in cold weather that disable the Li-ion transfer and increase the resistance.

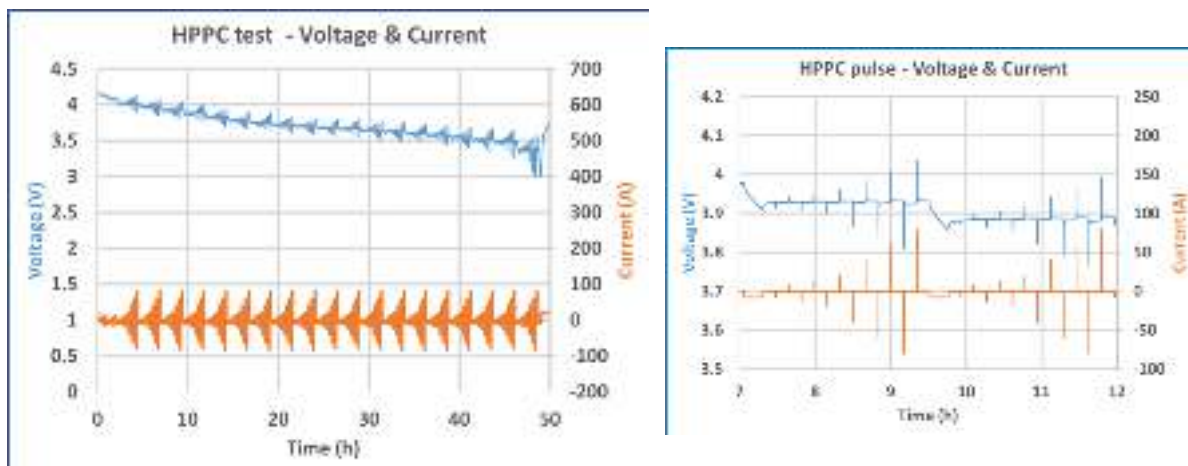
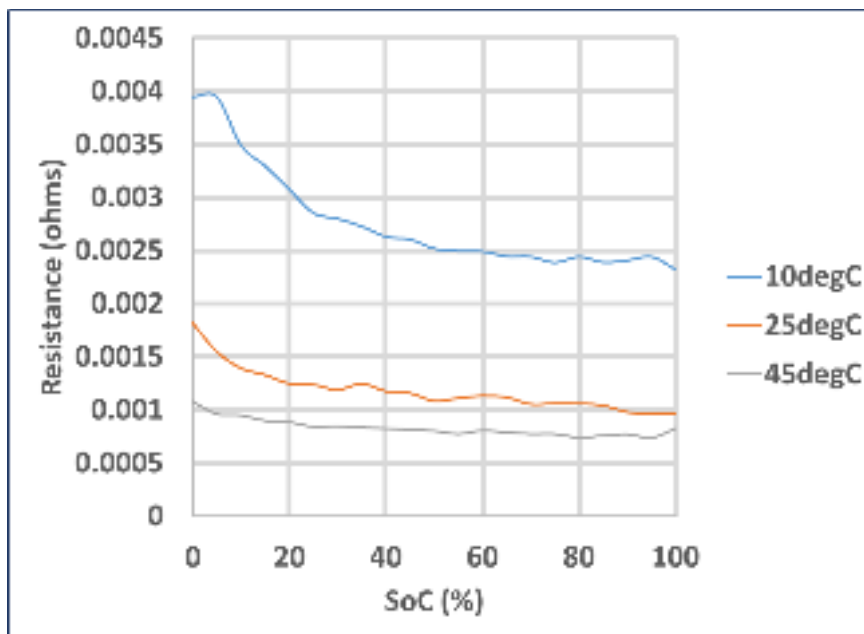


Figure 9. On the left: HPPC pulse train at 25°C with the current profile and voltage output response. On the right: example of a pulse train (closer loop).



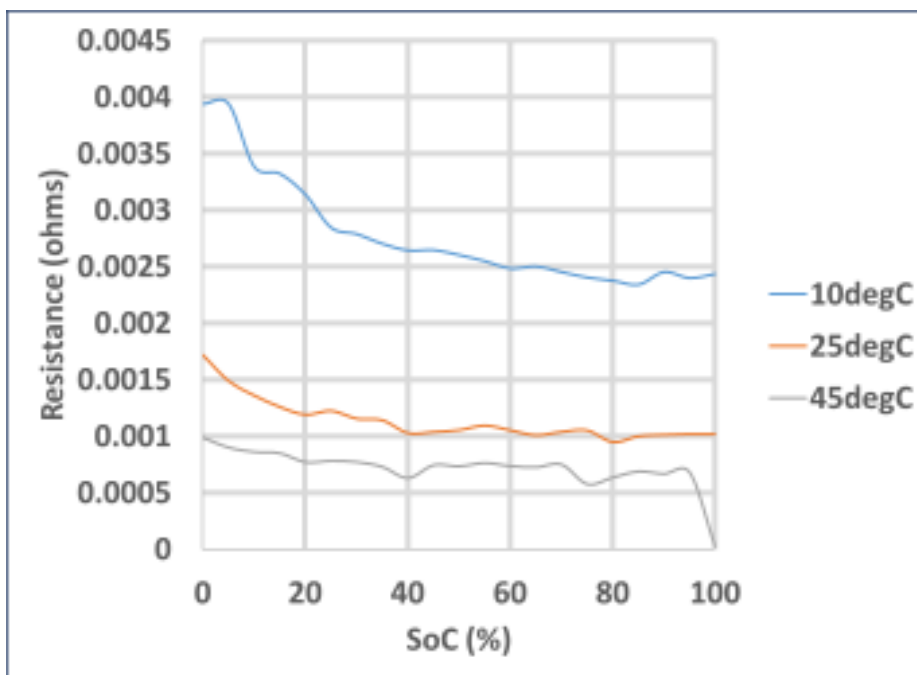


Figure 10. Internal resistance evolution at different temperatures for a discharging (top) and charging (bottom) state at C/5

3.1.4. Results from the electrical validation tests

The WLTC profile used for validation is presented in Figure 11. The measured cell voltage response during this test will be compared to the simulated voltage of the cell in the next section for validation purpose. This test has been performed at different temperatures for the complete validation of the model.

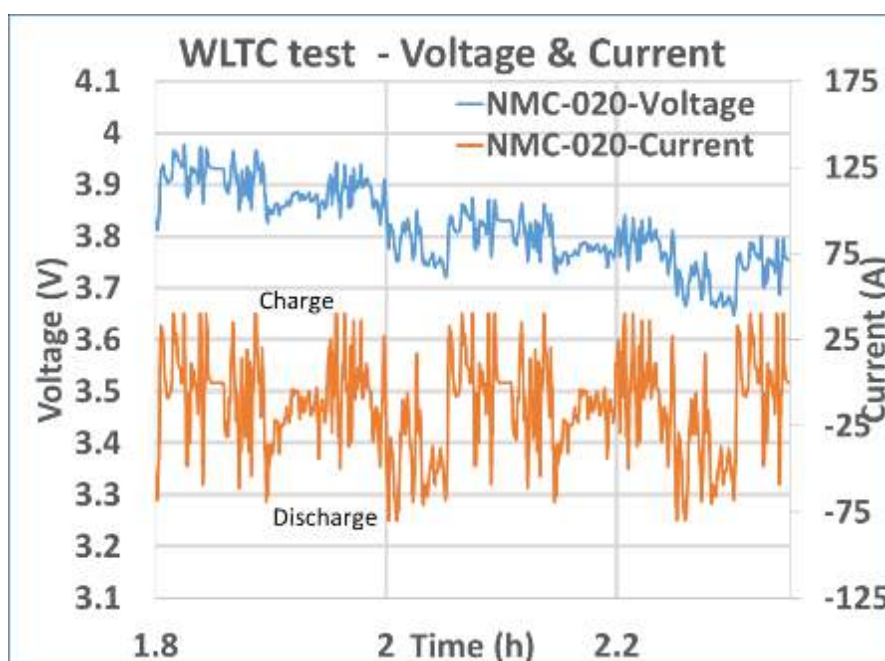


Figure 11. WLTC profile as a function of temperature

3.2. Results from standard data collection for thermal modelling

3.2.1. Temperature measurement

For every test, a maximal allowable temperature is defined to prevent gassing and critical failure of the cell resulting from overheating and thermal runaway. Also, the evolution of the temperature is an important parameter for designing a thermal model. Thus, it is necessary to have a reliable way of measuring battery temperature.

Because only one point of the battery can be measured for temperature, this point has to be carefully chosen. As reported in the literature [Goutam 2014] [Goutam 2015], the maximum temperature observed during cycling for NMC-based pouch cell is located near the positive tab.

Additionally, it is also visible from the IR images displayed in Figure 12 that the hottest point is mostly located near the positive tab of the cell for a C/2 discharge at 45°C. Therefore the k-type thermocouple will be placed on this spot during the thermal characterization.

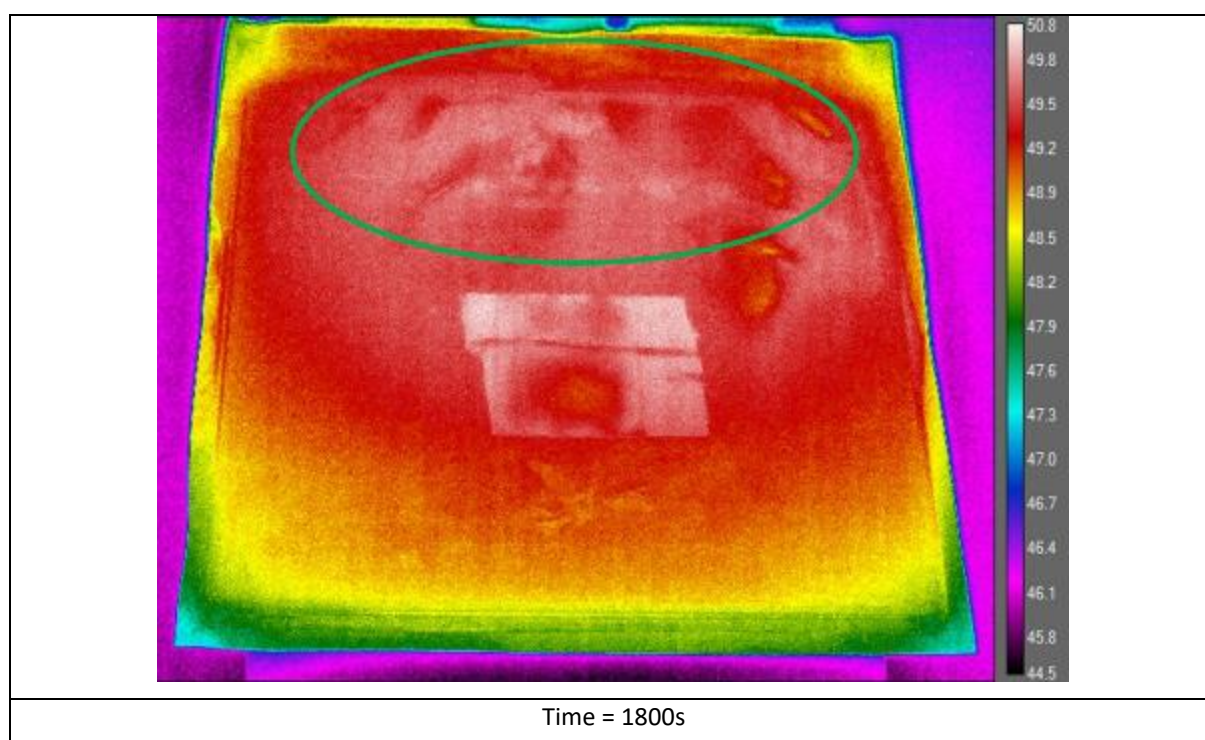


Figure 12. Temperature point for the NMC Kokam cell at different time intervals

3.2.2. Thermal validation tests

In order to correctly validate the thermal model created (parameter values are acquired from the different characterization tests), the validation test consisted in discharging the cell with a high constant current of 2C (86A) from 100% to 0% of SOC and at three initial temperatures (10°C, 25°C and 45°C). The results of these validation tests are shown in Figure 13 for which the variation of temperature, called ΔT , is displayed in order to compare the 3 tests. ΔT is a way of expressing temperature differences when conducting temperature tests and is calculated by subtracting the current battery temperature with the ambient one. It is a good way to compare different temperature tests for which the ambient temperature is not the same.

One can see that the ΔT is lower at high ambient temperatures (45°C), the reason is that the resistance of the cell becomes lower in the high-temperature environment due to more active side reactions which translates to a lower heat generation since it is based mainly on the Joules effect (battery resistance is lower at higher temperatures).

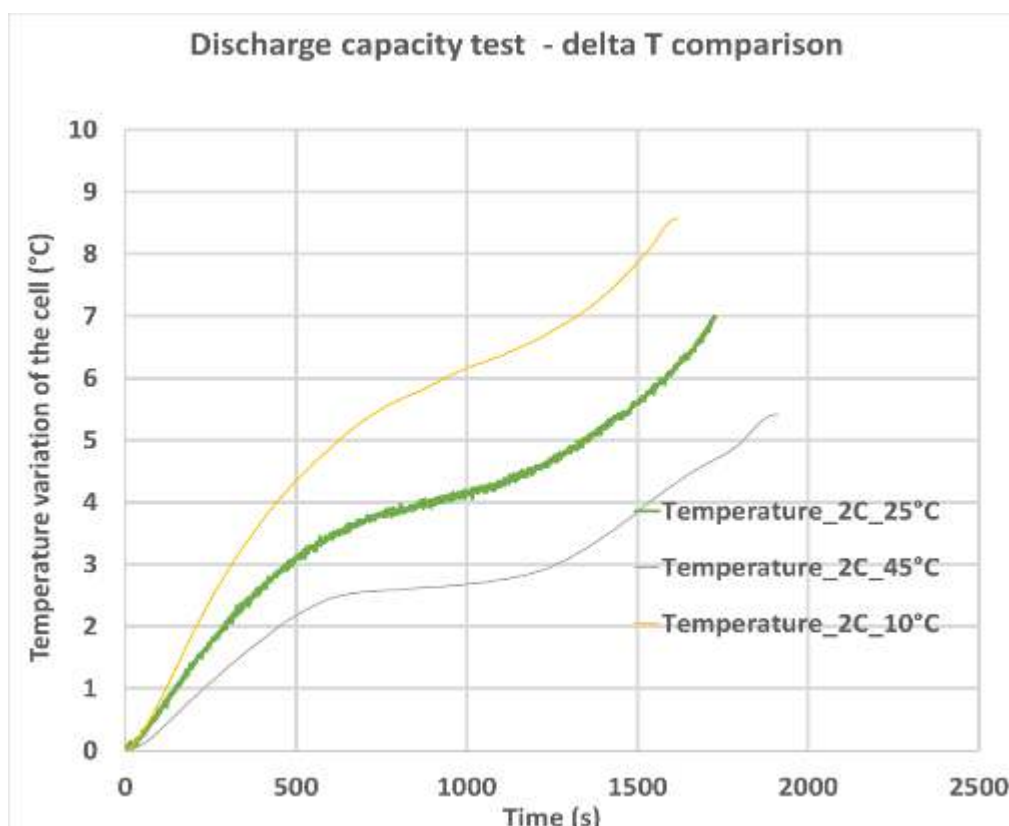


Figure 13. Temperature variation at 2C for a constant discharge test.

3.3. Conclusion on the characterisation

In this section, a detailed understanding of the electro-thermal behaviour of the NMC 40 Ah Kokam battery has been proposed. VUB characterization techniques in electric-thermal characterization have allowed in creating a good set of electrical and thermal parameters which can be implemented to perform electric and thermal model activities. The results of the electric-thermal characterization tests highly influence the outputs of the battery model. The type of tests is always the same but the difference comes in by way of careful implementation of the test itself, battery connections and intricate modifications in the test protocols. Such dedicated modifications have led to the creation of a qualitative set of electro-thermal characterization tests at different C-rates, SOC levels, and temperatures. The results of the characterization test of the NMC chemistry of the PANDA project were as expected and match with the general information provided by the manufacturer datasheet. In the coming section, the validation of these parameters will be presented in a modelling study for which a 1D-electro-thermal model is developed.

4. Electro-thermal modelling results of the NMC cell

In this section, it is demonstrated how the cell electro-thermal parameters obtained from the previous experimental work can be used to effectively model the voltage behaviour and the surface temperature of the cells under various scenarios. Modelling the cell temperature during operation is often required to ensure the cell is kept within the required temperature limits and also to calculate the cooling power required for thermal management application.

4.1. Description of the used methodology

In this study, a 1D-electro-thermal model is used. The model is based on the semi-empirical approach in a MATLAB/Simulink® interface. The aim of the model is to reproduce the cell's electrical and thermal performances with two parts: the electrical and thermal parts, as shown in Figure 14. The first part deals with voltage response calculation with the electrical parameters. The second one estimates the cell temperature based on the heat generation equation. This methodology for the lithium-ion cell thermal model has repeatedly been used in the literature with success and will therefore be adopted.

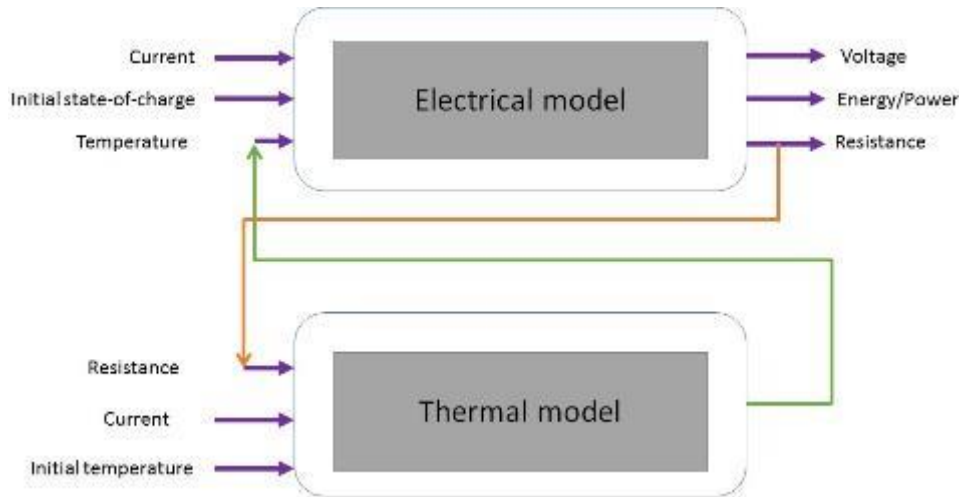


Figure 14. Schematic of the modelling methodology

4.2. Development of the electrical model

4.2.1. Description of the electrical model

The electrical model is built on the 1st order Thevenin model [Huria 2012] (See Figure 15) and consists of a voltage source with an ohmic resistance and a parallel RC circuit. Based on the equivalent circuit model, the battery output voltage of the Li-ion cell is the voltage drop resulting from the battery open-circuit voltage (OCV), the battery ohmic resistance (R_0), and battery polarization impedance (R_1C_1 circuit). The output voltage of the cell is then calculated by [Huria 2012]:

$$V_{cell} = V_{oc} - R_1 I_1 - R_0 I_{batt} \quad (2)$$

where I_{batt} is the flowing current in the battery (A), and I_1 is the current passing in the polarization resistance (A). Next, the level of charge or SOC is determined by the coulomb-counting method and is defined as [Boulon 2008]:

$$SOC = SOC_0 - \frac{1}{C_{init}} \int I_{batt} dt \quad (3)$$

with SOC_0 the initial state-of-charge of the cell. C_{init} is defined as the initial capacity (Ah) and it is assumed to depend on temperature [Hoog 2017] and current:

$$C_{init} = f(T, I) \quad (4)$$

In equation (2), all the circuit parameters are defined through lookup tables with V_{oc} pulse tests that correspond to a specific SOC and temperature [Jaguemont 2016]. Based on these parameters the heat generation is calculated in the thermal part of the model.

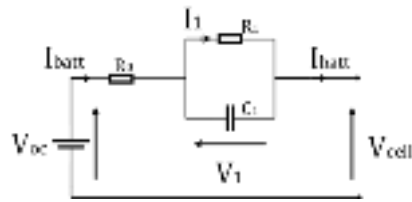


Figure 15: representation of the 1st-order Thevenin model

4.2.2. Results of the characterization for electrical modelling

The corresponding region of the electrochemical reactions at a current pulse is shown in Figure 16. In the left part of the figure, the HPPC is shown as an example of several short-duration current pulses at the various SoCs and C-rates. Also, in the right part of the figure, a zoom-in version is shown to associate the corresponding voltage to the current region. As it can be seen, the instantaneous overpotential from the OCV is due to the Ohmic region, estimated by R_o in our model, whereas the polarization effects are gathered to the rest V_1 , overpotential, dealing with charge transfer, diffusion capacitance, and concentration polarization effects.

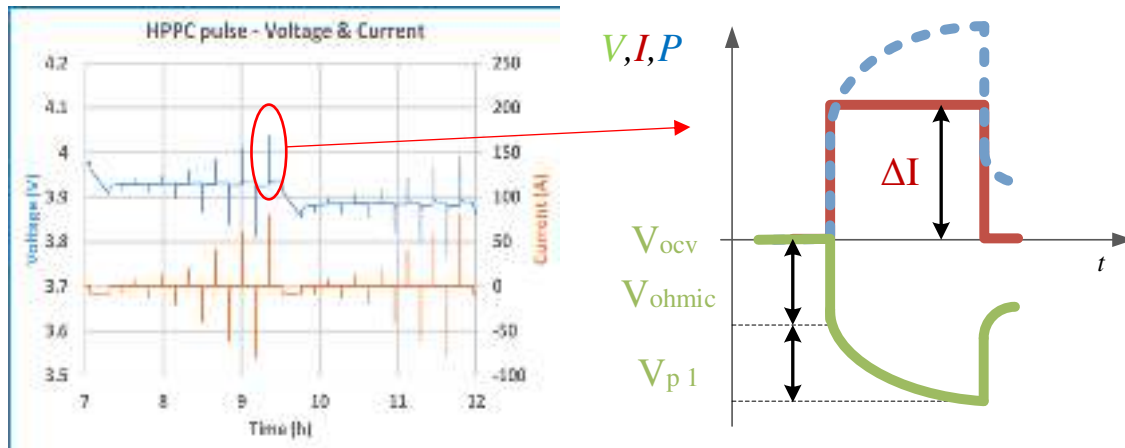


Figure 16. Left: HPPC pulses at certain SoC, Right: Corresponding region of the Thevenin ECM to the current pulses.

The model is characterized by extracting the electrical components values based on the equations describing the Thevenin ECM in time domain as shown below:

$$\begin{aligned} V_{cell}(t) &= V_{oc}(t) - R_1 I_1(t) - R_0 I_{batt}(t) \\ \frac{dV_1}{dt} &= -\left(\frac{1}{R_1 C_1}\right) V_1 + \left(\frac{1}{C_1}\right) I_{batt}(t) \quad (5) \end{aligned}$$

And discretised equations are:

$$\begin{aligned} V_{cell}(z) &= V_{oc} - R_1 I_1(z) - R_0 I_{batt}(z) \\ V_1(z+1) &= \exp\left(-\frac{t}{R_1 C_1}\right) V_1(z) + \left[1 - \exp\left(-\frac{t}{R_1 C_1}\right)\right] R_1 I_{batt}(z) \quad (5) \end{aligned}$$

As explained before, R_0 is the ohmic resistance, V_{ocv} is the open-circuit voltage, V_1 is the voltage at the battery terminals and the parallel RC branch represent the concentration and activation polarization (or charge transfer resistance) resistance R_{p1}/C_{p1} . Figure 17 to Figure 20 shows the electrical parameters for the 1st order model (see next section) extracted from the HPPC test for one cell, tested at 25 degrees. The figures show the resistances and time constant for the cell as a function of SOC and current rates separately for charge and discharge pulses.

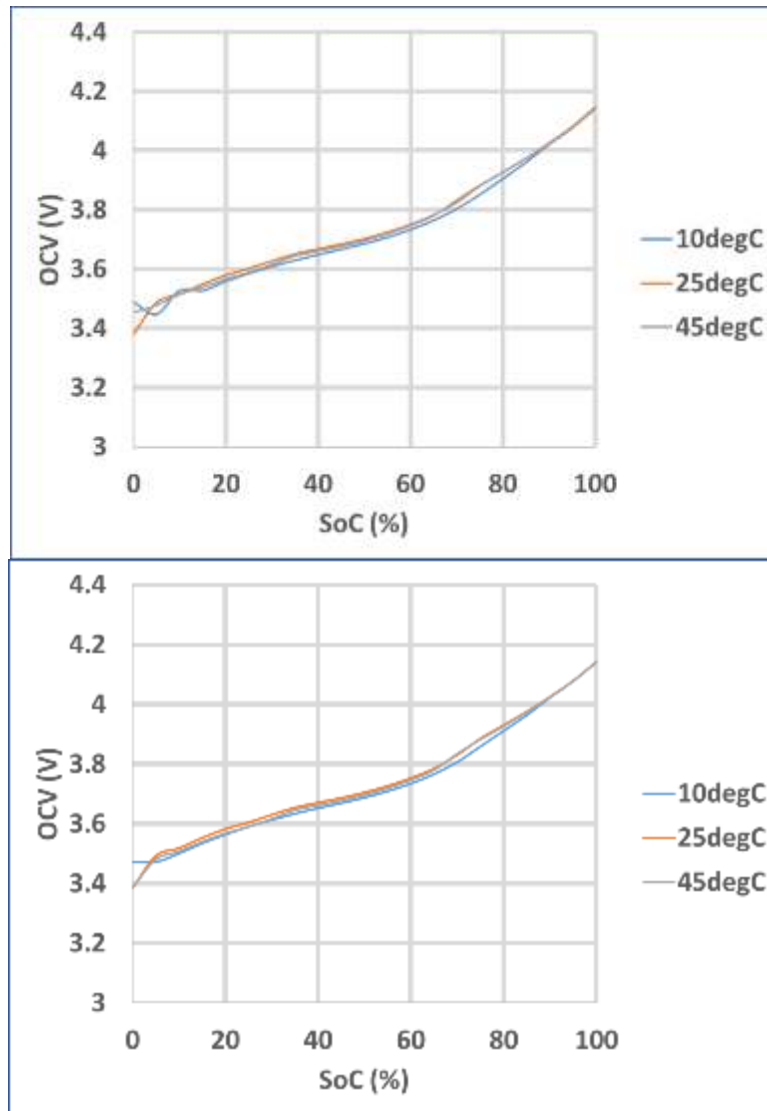
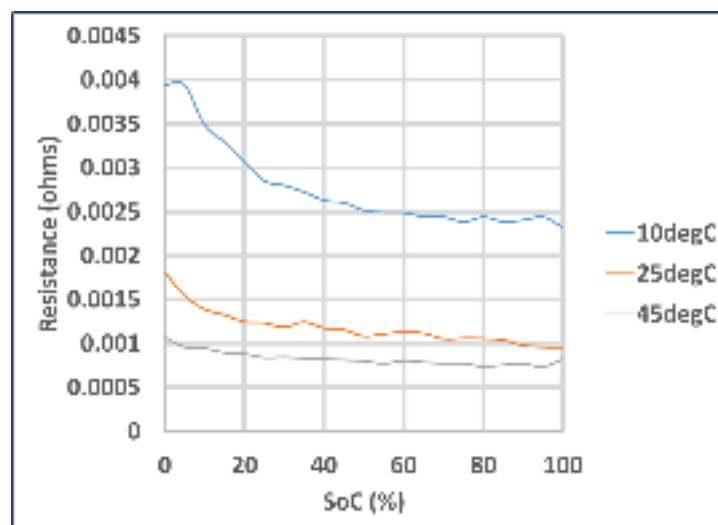


Figure 17. Discharge (top) and charge (bottom) OCV as a function of temperature and state of charge.



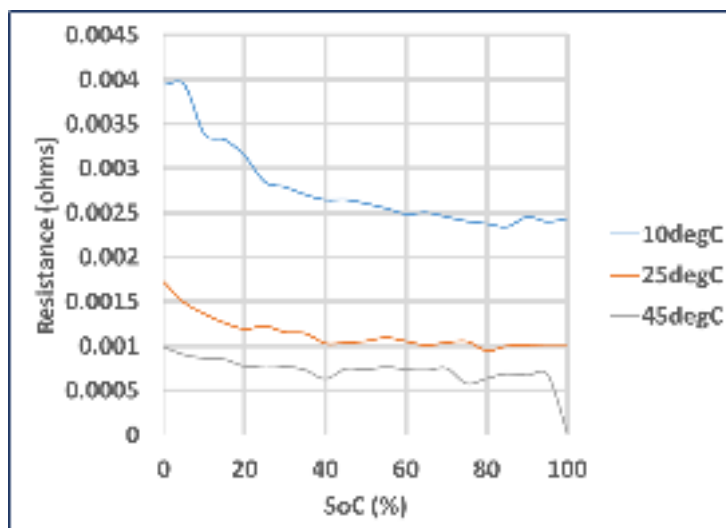


Figure 18. Ohmic resistance as a function of temperature and state of charge for the discharging (top) and charging states (bottom).

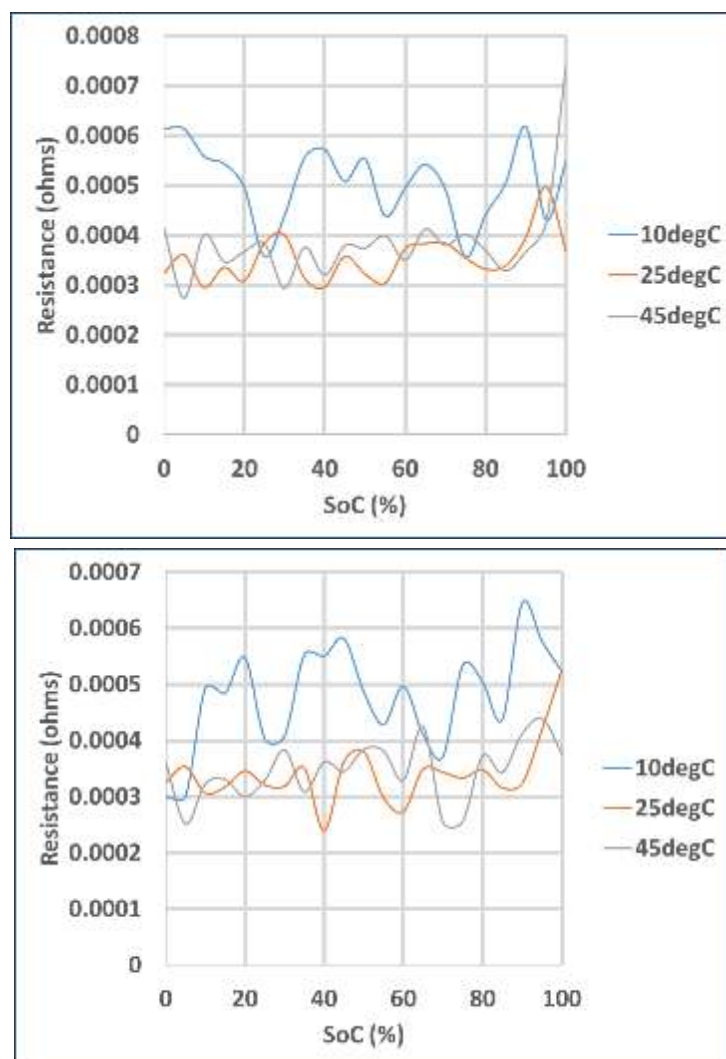


Figure 19. Polarization resistance as a function of temperature and state of charge for the discharging (top) and charging states (bottom).

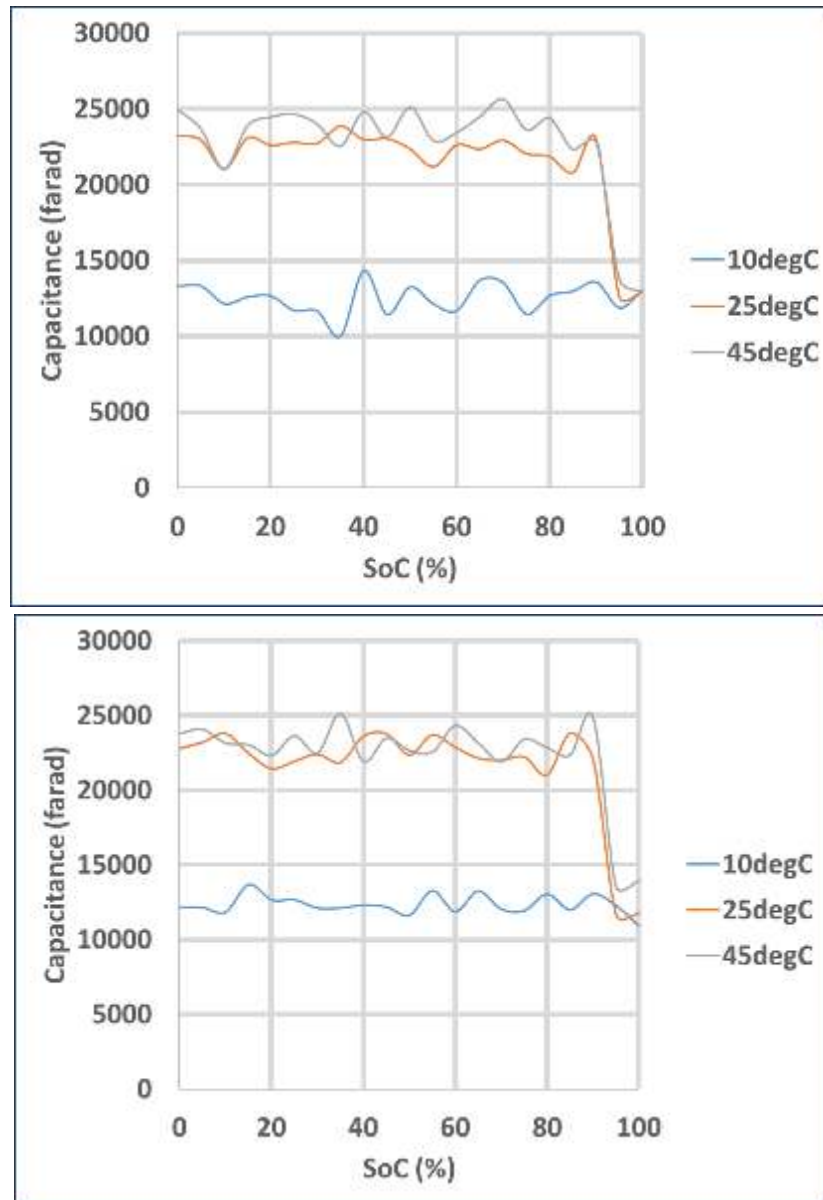
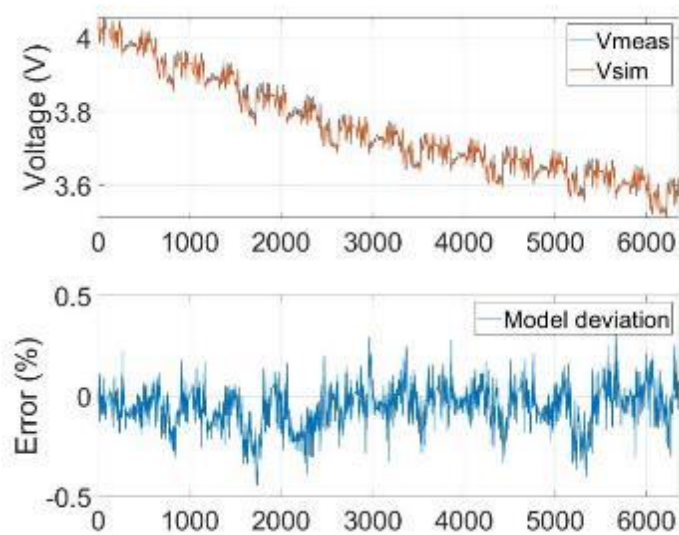
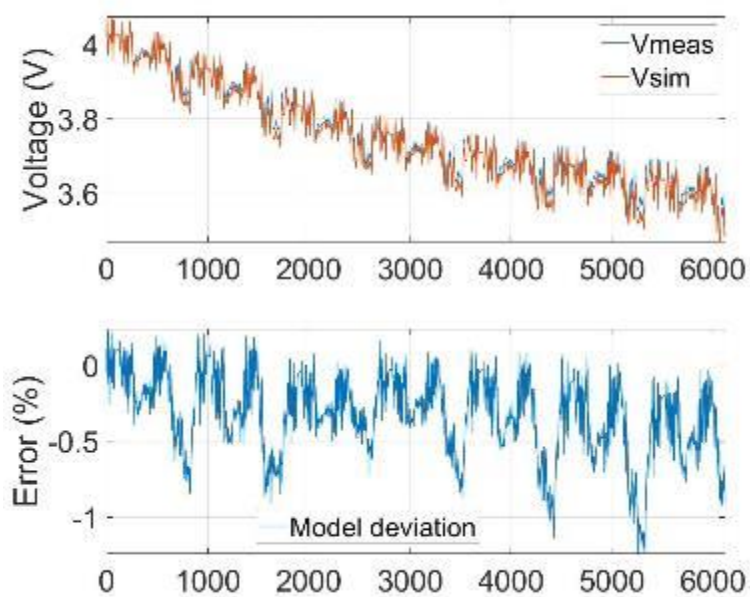


Figure 20. Equivalent capacitance as a function of the current rate and state of charge for the discharging (top) and charging states (bottom).

The parameters are extracted and collected into organized lookup tables which are a function of the state of charge, cell temperature and C-rate.

4.2.3. Results of the validation for electrical modelling

In order to correctly validate the electro-thermal parameters, some independent validation tests were performed accordingly to the validation profiles explain in the last section. Regarding the electrical part, the validation test consisted of applying a dynamic profile from 90% to 10% SOC to represent the electrical input of a BEV. The results of the validation for which the measured and estimated voltage for the cell under the loading condition at five temperatures: 10°C, 25°C, and 45°C are shown from Figure 21 to Figure 23. It is clear from the figures that the modelled voltage closely matches that of the voltage obtained during the electrical experiments hence providing further evidence of the authors' electrical modelling and the estimated electrical parameters. The error is calculated with the root-mean-square error (RMSE) for which the RMSE of simulation results is the deviation from the measurement data reflects the efficiency of the model for the capacity tests. Table 9 lists the model deviation for which a maximal of 2% error is depicted hence emphasizes the good modelling technique used in this report.



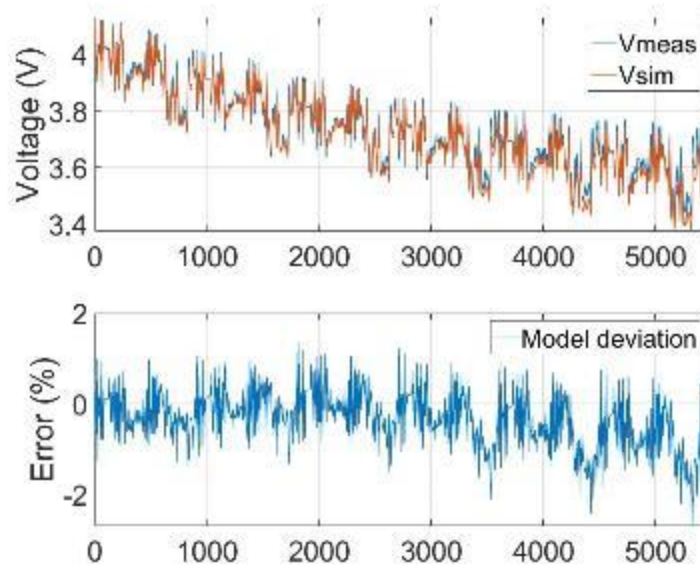


Figure 23. Validation of the NMC electrical model at 10°C.

Table 9. Electrical model deviation.

NMC electrical model deviation			
Temperature (°C)	10	25	45
Mean RMSE (%)	1.5	0.75	0.5

4.3. Development of the 1D-thermal model

4.3.1. Description of the 1D-thermal model

The thermal part of the model treats with the thermodynamics equations for prismatic-shape cells. In this part, as shown in Figure 24, heat is generated in a point located at the surface of the cell for which a specific heat capacity and a mass are found. The heat is then transferred from the surface of the cell to the ambient environment.

Conducting a heat balance equation at the point on the surface, the next equations obtained from thermodynamics [Incropera 2001], solve the heat transfer between the surface and the ambient:

$$\left\{ \begin{array}{l} \frac{dU_{cell}}{dt} = Q_{gen}(t) - Q_{loss}(t) = m \cdot C_p \cdot \frac{dT}{dt} \\ Q_{gen} = R_0 \cdot (I_{batt})^2 + R_1 \cdot (I_1)^2 \\ Q_{loss} = Q_{conv} = h_{conv} S_{area} (T_{cell} - T_{amb}) \end{array} \right\} \quad (6)$$

where U_{cell} , the internal energy, is the total energy contained by a thermodynamic system (J), Q_{gen} is the generating heating rate (W) in the corresponding element, and Q_{loss} is the heat losses of the corresponding element (W). C_p is the specific heat of the cell (kJ/kg.K) and m is the mass of the cell (kg), S_{area} (m²) the area of heat exchange, and the convective heat transfer coefficient h_{conv} (W/m².K).

The following assumptions are made for the thermal model:

The temperature of the surface of the cell, T_s is assumed to be uniform and therefore it represents the temperature of the whole cell. As the cell is a pouch the surface temperature and the internal temperature of the cell are considered close.

In this paper, heat generation is characterized only by ohmic losses, because the largest heat source in the battery operation comes from the ohmic resistance [Zhang 2011].

In the steady-state of thermodynamics, resulting from the temperature being constant, the amount of generated heat is the same as the heat losses, therefore equation 4 becomes:

$$\bullet \left\{ \begin{array}{l} 0 = Q_{gen}(t) - Q_{loss}(t) \\ Q_{gen} = R_0 \cdot (I_{batt})^2 + R_1 \cdot (I_1)^2 \\ Q_{loss} = Q_{conv} = h_{conv} S_{area} (T_s - T_{amb}) \end{array} \right\} \quad (7)$$

Natural convective heat transfer is considered in this paper with the following definition: T_{amb} . In this context, regarding the boundary limits of the model, the heat transfer with the surroundings is determined by following the convection equation

$$Q_{loss} = S_{area} \cdot h_{conv} \cdot (T - T_{amb}) \quad (8)$$

with S_{area} the exposed area (m²) and h the convection transfer coefficient (W/(m².K))

There are therefore two unknowns in Equation (5), C_p the heat capacity and h_{conv} the convective heat transfer coefficient. In this context, these two parameters are being determined based on a parameter estimation methodology described in the next section.

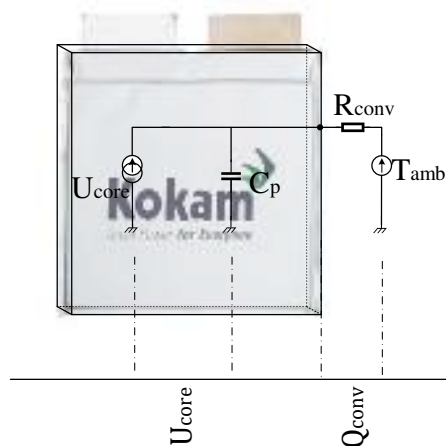


Figure 24: Overview of the thermal model with a thermal modelling schematic for the NMC Kokam cell.

4.3.2. Results of the characterization for thermal modelling

The specific heat capacity (C_p) and convective heat transfer coefficient (h) of the cells are important for the thermal model. To obtain them, a fitting technique using a fitting model and a specific test is used. The dedicated test has been described in the previous section.

To obtain the convective heat transfer coefficient, equations (7) are used in the steady-state. For Q_{gen} , the average value of the heat generation of the test after 20 min is used. The heat generation is calculated with the electrical model described before and is 10 W for a 2C-micropulse test. The ambient temperature is fixed to the tested temperature (10°C, 25°C, and 45°C), as for the final battery temperature, is it extracted from the experimental results as the final temperature point after 20 min of the test.

Nonetheless, since it is difficult to estimate as it depends on many parameters and variables, the value of this coefficient changes constantly especially in a non-adiabatic chamber, therefore the coefficient gradient will not be reported in this report.

For the C_p , the same experiment as above is used but in the transient state where the temperature of the cell presents a clear evolution. The least-squares regression of equation (8) is used to fit the surface temperature in a fitting model with the pre-defined value of h . The least-squares regression described above is also repeated at other temperatures to find thermal gradient behaviour. The specific heat capacities obtained with the method explained above are presented in Figure 26. From this figure, one can see that there is a positive correlation of the cell-specific heat capacity for the NMC cell with its temperature. Over the full temperature range subjected to the cell core, the average value of the specific heat capacity is 1000 kJ/(kg.K) for 50% of SOC.

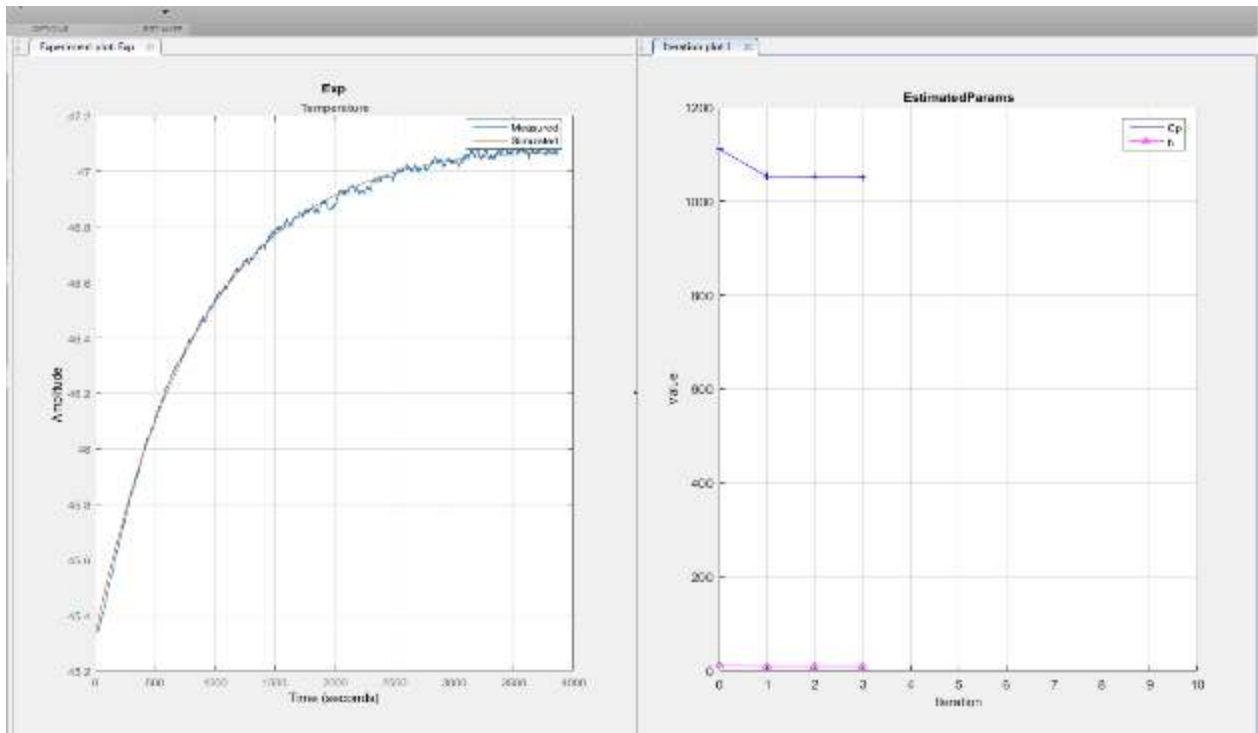


Figure 25. Example of the fitting curve exercise at 25°C where the fitted temperature curve has been created using Equation (7).

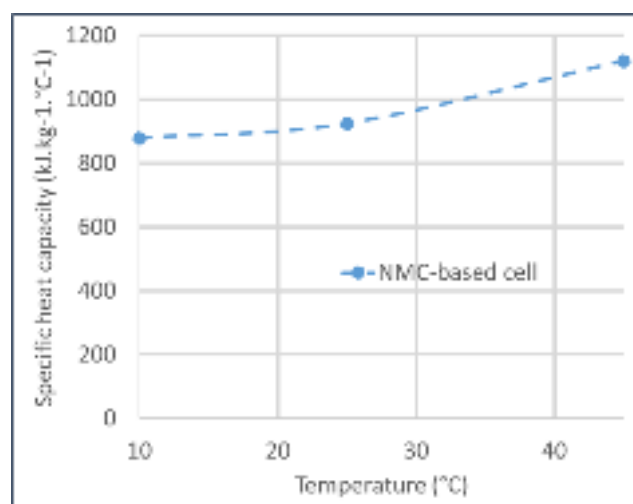


Figure 26. NMC specific heat capacities at different temperatures and at 50% of SOC.

4.3.3. Results of the validation for thermal modelling

The validation test of the thermal model consisted of discharging the cell with a high constant current of 2C (80A) from 100% to 0% of SOC and at five initial temperatures (10°C, 25°C, and 45°C).

The graph in Figure 27 has been realized using the values for C_p given in the last section and simulated using the model described in the previous section. It can be observed that though only ohmic heat generation is treated, the model accurately predicts the surface temperature.

As a result, the good model agreements of the electrical and thermal behaviours with experimental results also underline the validity of the model. Moreover, this validation provides robust evidence of the authors' heat capacity assessment as well the 1st Order Thevenin model discussed earlier.

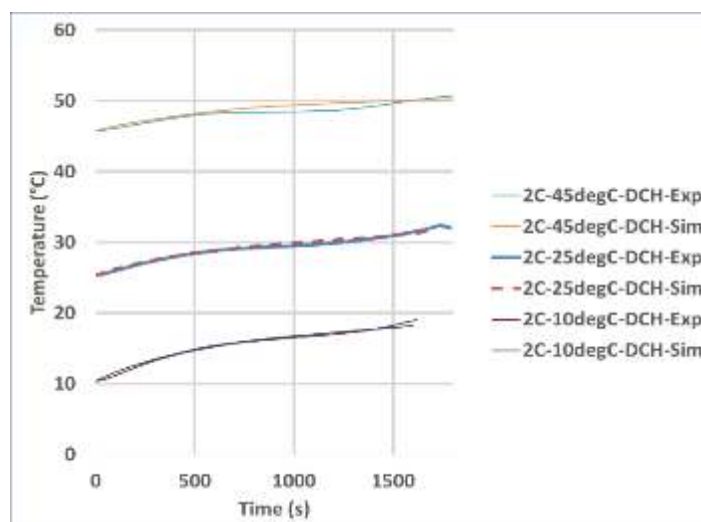


Figure 27. Validation of the NMC thermal model at different initial temperatures.

4.4. Conclusion on the 1D-electro-thermal modelling

The proper simulation of lithium-ion batteries in today's automotive and electric applications is of great importance for efficient use and correct understanding of the electrical, thermal, chemical behaviour of the system under investigation. Different models exist in the industry and literature, each having their own advantages and disadvantages. In this section, the development of a 1D-electro-thermal and the voltage behaviour under static and dynamic load profiles of 40Ah pouch cells is presented. The model, based on Matlab/Simulink was elaborated on NMC cell. The experimental results used for validation showed a temperature estimation to be fairly uniform after a complete discharge with 2°C of maximal temperature

difference. In addition, from the comparison of both simulations and the experimental results, a good agreement was found with a maximum error of 2 % and 2°C for the electrical and thermal. Additionally, the validation has been done at three initial temperatures (10°C, 25°C, and 45°C) which means that a solid foundation for the generalized model methodology of PANDA is provided.

5. Development of the NMC battery pack model in Matlab / Simulink

In the framework of the PANDA project, different cases will be studied. One of them is the Renault Zoe use-case for which a BEV is available and with an instrumented vehicle and 32 km of different road profiles for driving tests. In order to check the interest of the proposed method in WP2 on an actual BEV, the Zoe driving data will be used.

In this section, we present the validation of the Matlab / Simulink methodology with the Zoe data provided by RTR. As the data are classified as confidential, all the information presented in this section is obtained from the Renault company website (<https://fr.renault.be>) and online available presentations (http://cii-resource.com/cet/AABE-03-17/Presentations/BMGT/Delobel_Bruno.pdf) [Delobel 2017].

5.1. The structure design of the PANDA P-HEV battery pack

The Renault Zoe (sometimes stylized as ZOE and pronounced as "Zoé") is a five-door supermini electric car produced by the French manufacturer Renault. To propel the vehicle, Zoe has a 41 kWh lithium-ion battery pack (https://en.wikipedia.org/wiki/Renault_Zoe) that delivers a range between 400 km under the NEDC cycle (https://en.wikipedia.org/wiki/Renault_Zoe). The battery pack is structured as followed:

- Total weight: 305 kg
- Available capacity: 41 kWh
- Cells: 192 cells, each with 63Ah nominal capacity and 3.75 V nominal voltage

A picture of the Zoe battery pack is shown in Figure 28:



Figure 28. The structure design of the 360V Zoe battery pack with 12 modules.

5.2. Battery pack model methodologies

Starting from the Zoe battery pack data, we propose to develop a battery pack using the previous parameters upscaled to series and parallel connections.

There are different approaches to build a battery pack model ordered according to their level of complexity:

- cell-level aggregation model,
- generic battery model,

Cell-level aggregation model: in this method, the number of cells composing the battery pack requires the same amount of cell-level models as in the defined topology. This means that different parameters for each cell level

model are considered. Also, a loss of fidelity and increase in model deviation when complex topologies are considered is often observed.

Generic battery model: this method is the fastest and consists of scaling up the cell-level model using one cell-level model for which the available capacity values, the current, mass and total voltage are multiplied by the number of series and parallel strings. Nonetheless, discrepancies can be created as the same cell-level parameters are used to model the complete module.

5.3. 1D-electro-thermal model development of the pack

In the context of the Zoe battery pack development, we propose to use the generic battery model approach as it is the fast method. Figure 29 shows the adapted battery system in the Matlab / Simulink environment.

The electrical model is built on the 1st order Thevenin model [Hurria 2012] and in order to consider the battery pack voltage, the voltage of one cell is multiplied by the number of series connections (ns). Regarding the battery pack current, I_{exp} , it is divided by the number of parallel connections to relate it to a single-cell. It is assumed that the current is equally distributed among the cells.

The output voltage of the pack and the input current are then calculated by:

$$\begin{cases} V_{pack} = V_{cell} \times ns \\ I_{cell} = \frac{I_{exp}}{np} \end{cases} \quad (9)$$

with ns the number of strings in series; I_{exp} , the experimental driving profile (A) and np the number of strings in parallel

Concerning the thermal model, the battery pack is considered as a single thermal component with one temperature point. This means a global heat generation, specific heat capacity and convective coefficient are considered, only the mass is multiplied by the total number of cells, assuming that Joule losses are equally generated from all cells. Therefore, the equations solving the heat diffusion in the pack are the following:

$$\begin{cases} \frac{dU_{pack}}{dt} = Q_{gen}(t) - Q_{loss}(t) = m_{pack} \cdot Cp \cdot \frac{dT}{dt} \\ m_{pack} = m_{cell} \times n \\ Q_{gen} = R_0 \cdot (I_{batt})^2 + R_1 \cdot (I_1)^2 \\ Q_{loss} = Q_{conv} = h_{conv} S_{area} (T_{cell} - T_{amb}) \end{cases} \quad (10)$$

with n the number of cells composing the pack and m_{pack} the total mass of the battery system (kg). S_{area} is the external surface of the pack and Q are the heating powers (W).

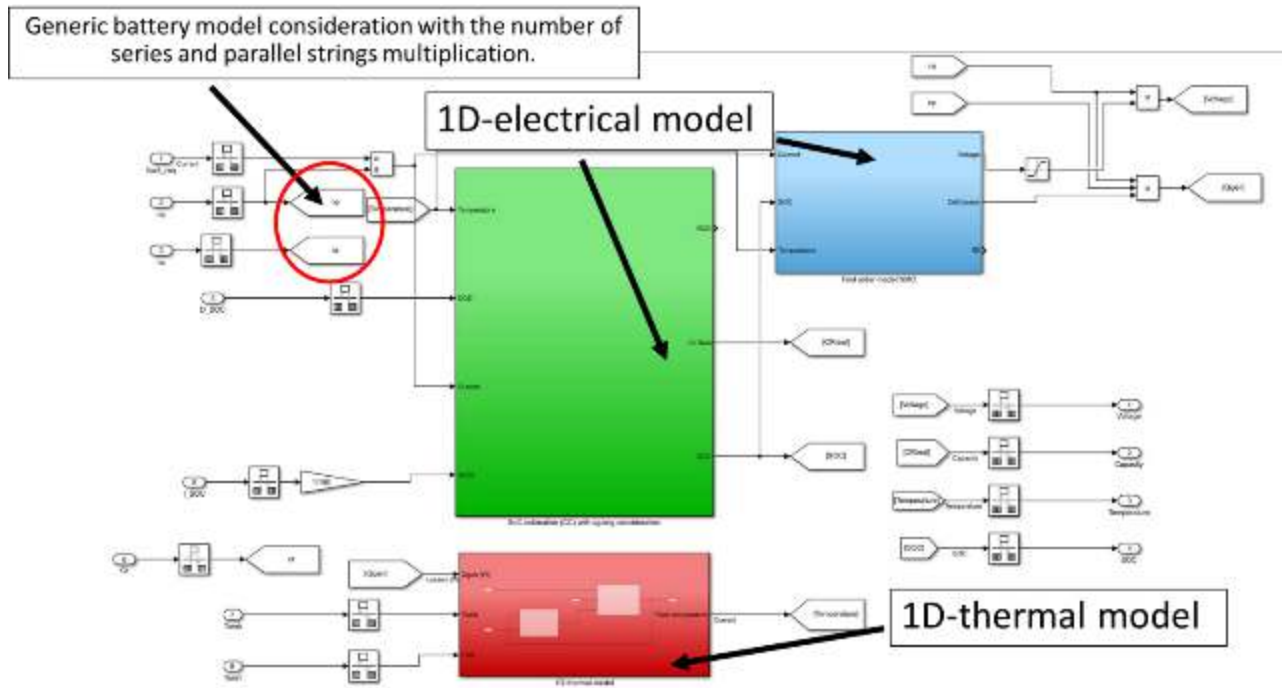


Figure 29. Matlab / Simulink model of the battery pack system.

5.4. Validation results

In order to correctly validate the battery pack model, RTR recorded the voltage and temperature outputs on a typical driving profile. The information on the current profile will be disclosed in this report as the deliverable is destined for a public version.

Nonetheless, the measured pack voltage and temperature responses during this test will be compared to the simulated voltage and temperature of the system in this section for validation purpose. This test has been performed at ambient temperature (25°C).

The validation test consisted of applying a driving profile to represent the electrical input of the Zoe. The results of the validation shown in Figure 30, displays the measured and estimated voltage for the cell under the loading condition at ambient temperature.

As shown in the figure, the modelled voltage closely matches that of the voltage obtained during the electrical experiments, hence providing further confirmation that the authors' electrical modelling and the generic battery pack approach is correct. The error is calculated with the root-mean-square error (RMSE) for which the RMSE of simulation results is the deviation from the measurement data reflects the efficiency of the model for the capacity tests. Table 10 lists the model deviation for which an average of 1% error is depicted, hence emphasizes the quality of the modelling technique used in this report.

In addition, the temperature during the driving profile was recorded. The graph in Figure 31 has been realized using the values for C_p given in the last section and the generic battery pack model approach. It can be observed that though only ohmic heat generation is treated, the model accurately predicts the surface temperature.

As a result, the good model agreements of the electrical and thermal behaviours with experimental results also underline the validity of the model.

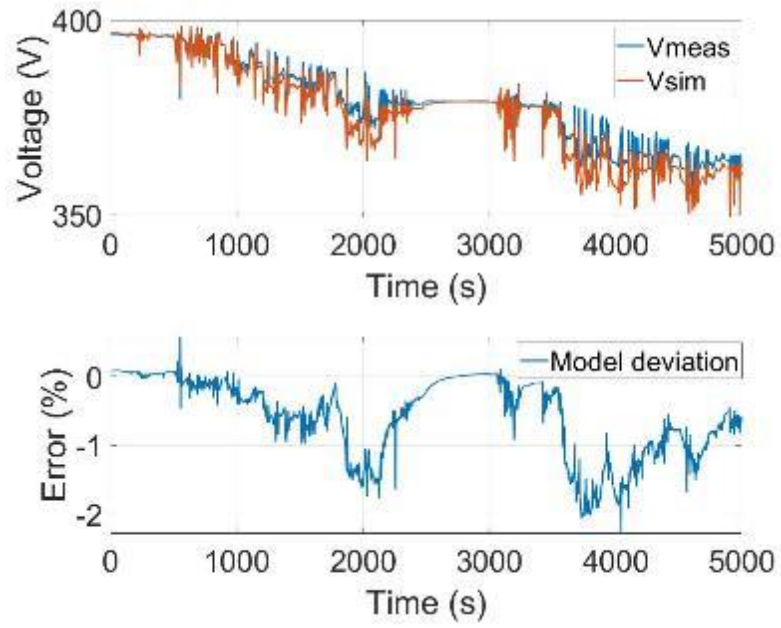


Figure 30. Validation of the NMC electrical model at 25°C.

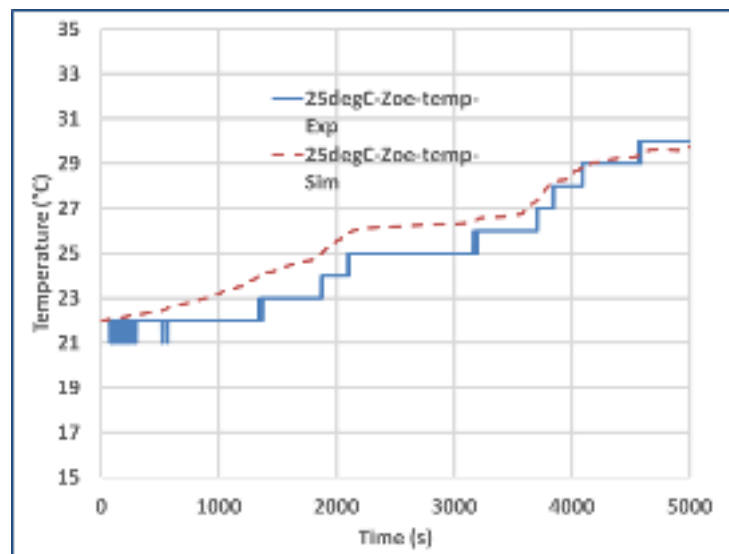


Figure 31. Validation of the NMC thermal model at different initial temperatures.

6. Development of the NMC battery pack model in Matlab using EMR

In this section, the organization of the electro-thermal model using Energetic Macroscopic representation (EMR) by the University of Lille [Bouscayrol 2012]. From previous work on EMR of batteries [German 2019], this organization in Matlab /Simulink environment is presented. In a second time, the EMR model of the battery pack is developed and model in Simcenter AMESim environment thanks to the EMR library developed in this simulation package [Husar 2019]

Table 10 is a summary of the parameters used in the electro-thermal model with the variables they are depending on. Figure 32 shows the coupling principle of the electro-thermal model with an update of the electrical parameters as a function of the current, the SoC and the temperature of the cell.

Table 10: Dependence of the model parameters.

	Parameter	Name	Unit	Dependence
Electrical	OCV_{Cell}	Open circuit voltage	(V)	$SOC_{Cell}, T_{Cell}, i_{Cell}$
	R_{0Cell}	Cell series resistance	(Ω)	
	R_{1Cell}	Cell relaxation resistance	(Ω)	
	C_{1Cell}	Cell relaxation capacitance	(F)	
Thermal	R_{ThCell}	Thermal resistance of the cell	(K/W)	Constant
	C_{ThCell}	Thermal capacitance of the cell	(J/K)	

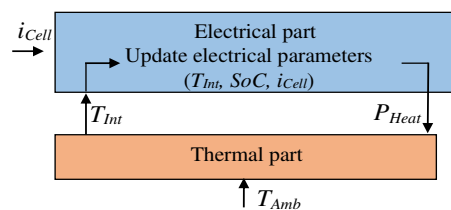


Figure 32. Electro-thermal coupling principle.

6.1. Validation results

As shown in Figure 33, EMR is based on [Bouscayrol 12]:

- pictograms (one pictogram is representing one function (see appendix)),
- power (the action and the reaction variables between two pictograms must yield to a power variable,
- compulsory integral causality.

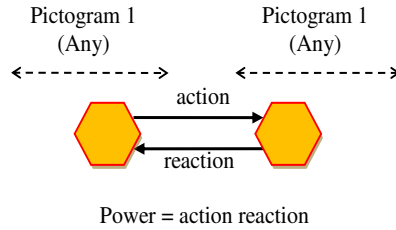


Figure 33. The power exchange between pictograms.

6.2. EMR representation of the battery pack model

6.2.1. Reorganization of the Simulink electro-thermal model for the single-cell

In particular, the entropy flow (W/K) is introduced. The EMR variables are listed in Table 11:

Table 11: EMR variables for electro-thermal modelling.

	Parameter	Name	Unit
Electrical	u	Voltage	(V)
	i	Cell series resistance	(Ω)
Thermal	q_s	Entropy flow	(W/K)
	T	Temperature	(K)

The second consequence is the reorganization of the governing equations (2-8) according to the EMR elements which are presented in Appendix A, Table 13. The EMR for a single-cell is displayed in Figure 34. The electrochemical storage (ECS), the current source and the air are energy sources (green oval pictograms) imposing their outputs (OCV_{cell} , i_{cell} and T_{Amb}) to the rest of the system.

R_{0cell} is a multi-domain (electro-thermal) coupling element (overlapped orange circles).

$$\begin{cases} u' = OCV_{cell}(SoC) - R_{1cell} i_{cell} \\ q_{SR0cell} = \frac{R_{0cell} \cdot i_{cell}^2}{T_{cell}} \end{cases} \quad (11)$$

The series connection is a mono-domain (electrical) coupling element (overlapped orange squares).

$$\begin{cases} u_{cell} = u' - u_{c1cell} \\ i_{cell} = i_{cell} \end{cases} \quad (12)$$

The parallel connection is a mono-domain (electrical) coupling element (overlapped orange squares).

$$\begin{cases} i_{c1cell} = i_{cell} - i_{R1cell} \\ q_{SR0cell} = \frac{R_{0cell} \cdot i_{cell}^2}{T_{cell}} \end{cases} \quad (13)$$

C_{1cell} is an accumulation element (crossed orange rectangle).

$$u_{c1cell} = \frac{1}{C_{c1cell}} \int_0^t i_{c1cell} dt \quad (14)$$

R_{1cell} is a multi-domain (electro-thermal) conversion element (orange circle).

$$\begin{cases} i_{R1Cell} = \frac{u_{C1Cell}}{R_{1Cell}} \\ q_{SR1Cell} = \frac{R_{1Cell} \cdot i_{R1Cell}^2}{T_{Cell}} \end{cases} \quad (15)$$

The thermal coupling a mono-domain (electrical) coupling element (overlapped orange squares).

$$\begin{cases} T_{Cell} = T_{Cell} \\ q_{STot} = q_{SR0Cell} + q_{SR0Cell} \end{cases} \quad (16)$$

C_{ThCell} is a an accusation element (crossed orange rectangle).

$$T_{Cell} = T_{Cellinit} \cdot e^{\frac{1}{C_{ThCell}} \int_0^t (q_{STotCell} - q_{S3}) dt} \quad (17)$$

R_{ThCell} is a mono-domain (thermal) conversion element (orange square).

$$\begin{cases} q_{S3} = \frac{T_{Cell} - T_{Amb}}{(R_{ThCell}) \cdot T_{Cell}} \\ q_{S4} = \frac{T_{Cell} - T_{Amb}}{(R_{ThCell}) \cdot T_{Amb}} \end{cases} \quad (18)$$

6.2.2. EMR of the electro-thermal model for one cell

Figure 34 presents the EMR of the electro-thermal model. EMR has the following advantages.

- The action/ reaction principle can be systematically checked (which can be difficult in a block diagram).
- The state variables (or dynamics) are highlighted by accumulation element outputs.
- The different interactions between electrical and thermal parts are highlighted.

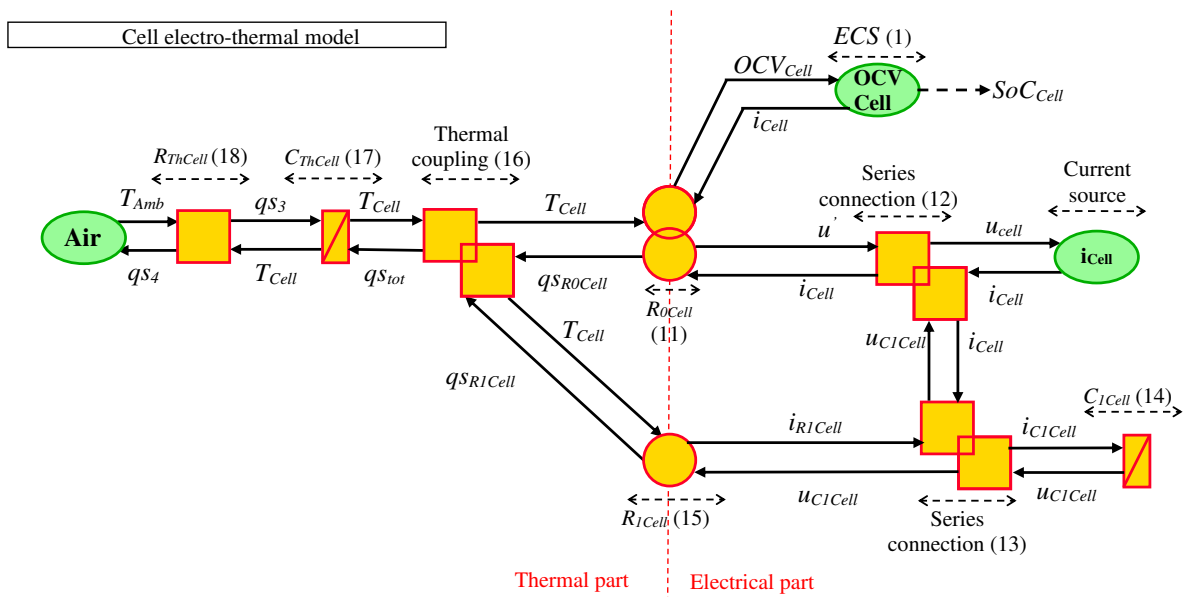


Figure 34. EMR of the dynamical electro-thermal model for a single cell.

6.2.3. Comparison of the two representations (block diagrams and EMR)

As the model methodology is the same for both representations (block diagrams and EMR), this subsection compares the outputs results applying the same inputs. The test was done by comparing u_{Cell} and T_{Cell} for an input current (Figure 35) corresponding to a WLTC driving cycle and results are shown from Figure 36 to Figure 37. Moreover, the same initial conditions (SoC and temperature) are used, and as the physical causality is respected in both representations, the simulation time is the same.

Both models are simulated by using Matlab/Simulink and the same computer. The results shows two main aspcts.

- There is no model deviation in the output voltage and temperature curves

- The simulation times are comparable (no significant difference).

In the end, EMR is just a way to reorganize the same model in a more systematic and physical approach. Because it is the same model, both representations give the same results. As EMR is the common tool of the PANDA project, the battery model is in agreement with other sub-systems models developed within this project. Thus, it can be easily interconnected.

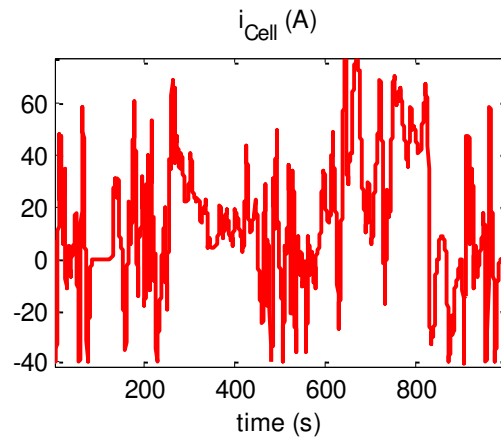


Figure 35. Evolution of the input current.

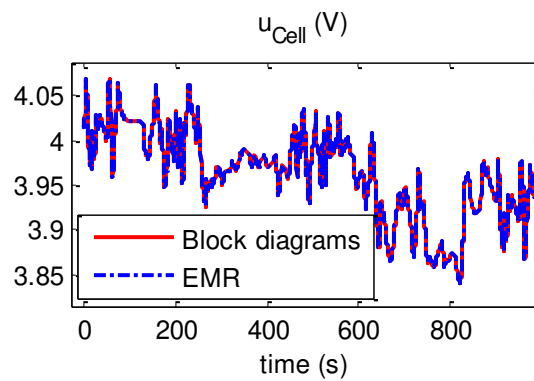


Figure 36. Evolution of the cell voltage.

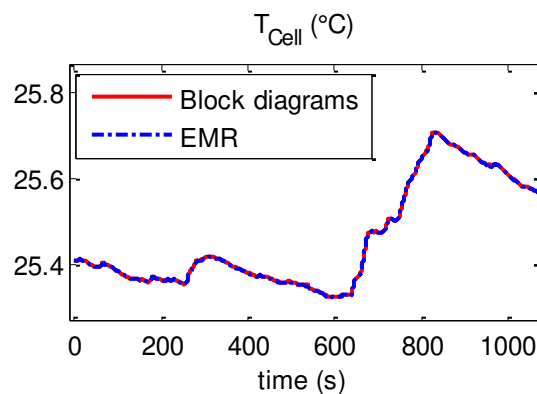


Figure 37. Evolution of the cell temperature.

7. Development of the NMC battery pack model in Simcenter Amesim using EMR

7.1. Simcenter Amesim Electric Storage (ESS) library

Simcenter Amesim has an Electric Storage (ESS) library whose objective is to accurately evaluate the energy exchanges of such devices in variable environmental conditions. Depending on those variations and the analysis to perform, ESS enables to model electric storage systems with various complexities and features. Representing their behaviour is especially interesting in multi-physics systems to specify the power and energy needs, size a battery pack, design a corresponding cooling subsystem or validate related control systems.

The aim of the ESS library is to model the electrical and thermal energy exchanges of electric storage systems. The energy state of those systems is only described by a few macroscopic quantities such as current, voltage, temperature or heat flow rate. This modelling approach is suited to study the energetic interactions of electric storage systems, with accurate results and fast simulation computations.

Various electrochemical phenomena are modeled with an equivalent electrical circuit. Equivalent parameters such as resistance, a time constant or efficiency coefficient are used to characterize the component models. This generic capability enables to represent different technologies with the same modeling structure. For example, NiMH batteries and Li-ion batteries can be modelled with the same components, but a different set of parameters needs to be used.

The internal dynamics of the electric storage system, as well as the interaction with the environment can be simulated in a multi-physics environment by using components from the Thermal, Electrical Basics or Electrical Static Conversion libraries for example.

7.1.1. Library content

The ESS library features models of batteries, ultra-capacitors and control units. Its display is shown in Figure 38. The components are sorted into subfolders:



Figure 38. Electric Storage library display.

All the component icons of the ESS library are shown in Figure 39.

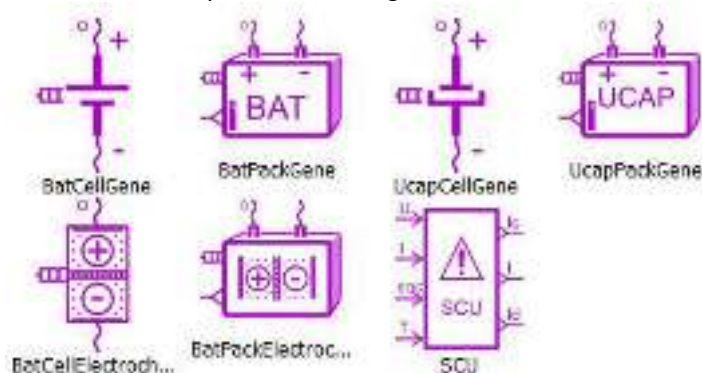


Figure 39. Electric Storage subfolder icon content.

The Batteries subfolder contains the battery component icons (Figure 40):

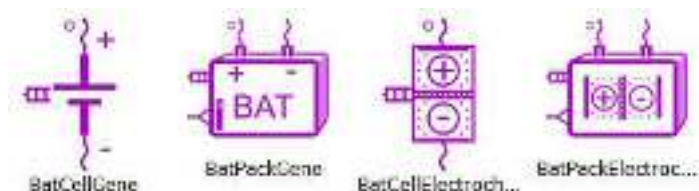


Figure 40. Batteries subfolder icon content.

7.1.2. Cell and pack models

Battery packs are made of several cells connected in series or/and in parallel, as illustrated in Figure 41:

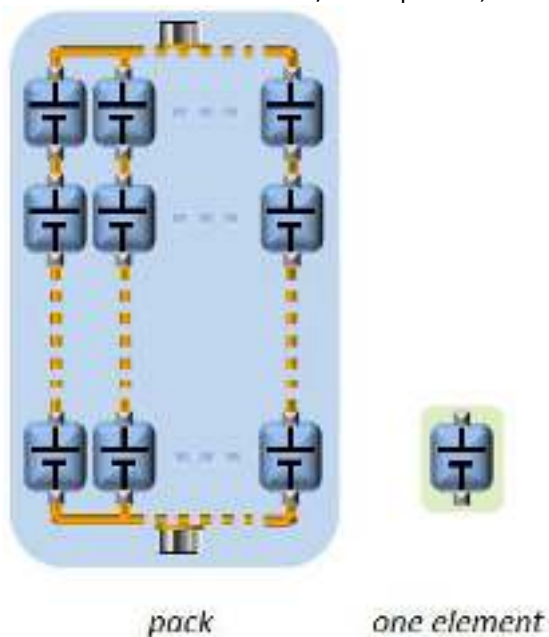


Figure 41. Cell and pack electrical connection.

The ESS library contains cell and pack components. Examples of cell component icons are given in Figure 42, they have 2 electrical ports and 1 thermal port:



Figure 42. Battery cell icon examples.

Examples of pack component icon are given in Figure 43. In addition to the 3 physical ports similar to the cell components, they have a signal port giving the pack state of charge as an output:

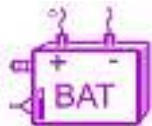


Figure 43.: Battery pack icon examples.

To model a pack, can either be used cell model which allows to individually model every cell in the pack or the pack model directly when all the cells in the pack are considered to be identical. For instance, the same battery pack could be described as 10 cells of 3.8 V connected in series, or as a 38 V pack. Figure 44 shows a sketch comparing a battery pack model with a set of battery cell models:

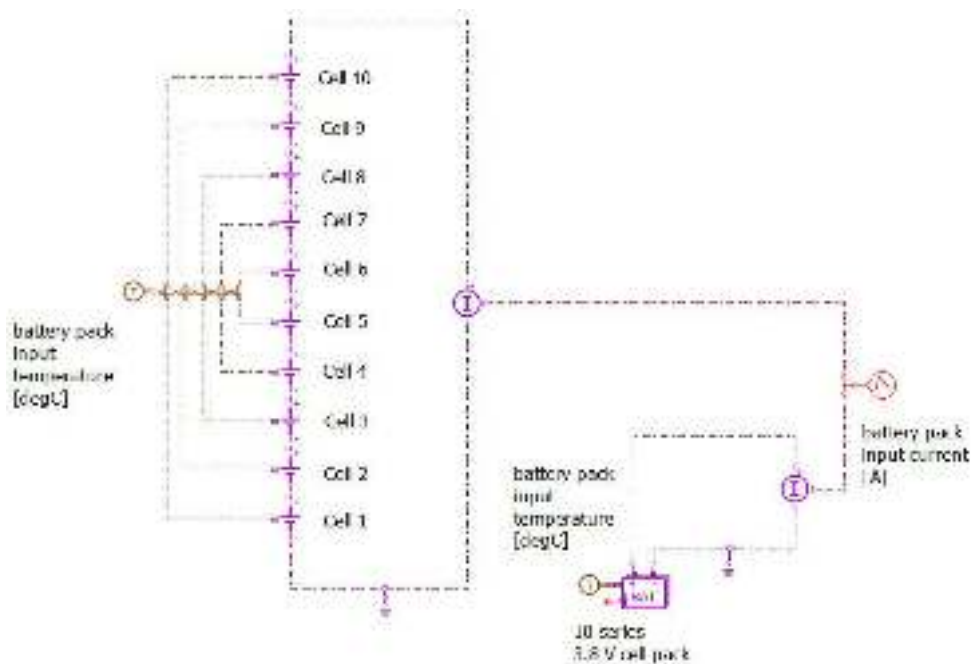


Figure 44. Battery pack and battery cell comparison model.

7.1.3. Notations and conventions

Electrical dipoles in the ESS library, such as batteries or ultracapacitors, use the passive convention. For every such component, the two internal variables input current and input voltage are defined, with the direction defined in Figure .

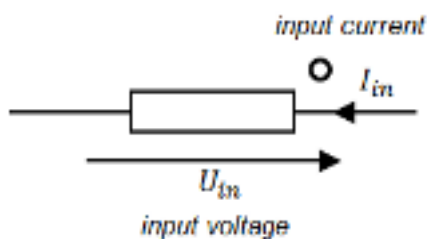


Figure 45. ESS dipoles use the passive convention.

A white dot is used on the icon using this passive convention, to indicate the electrical port defining the input current and input voltage variable direction (Figure 46).

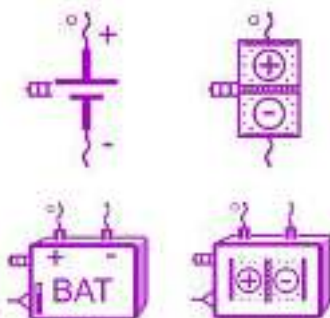


Figure 46. The passive convention is indicated with a white dot on the icons.

Many components use text parameters to define data files or expressions, for example for parameters such as a battery open-circuit voltage or internal resistance which can have a dependency with the state of charge, current or temperature.

7.2 EMR-based battery model in Simcenter Amesim

Simulation of batteries for automotive applications offer better testing procedures if the battery models are simulated as an integral part of the entire vehicle powertrain. Such system simulations offer better test environments which could better emulate real operating scenarios.

The NMC battery pack model based on the collaboration between WP2 and WP4, represent the first EMR battery model simulated within Simcenter Amesim. A reduced model of the one developed in section 4 and 5 will be implemented first in the EMR-based library of Simcenter Amesim: the battery model without its temperature dependence. The complete model will be integrated later (electro-thermal model). Thus, we will have two different models of the same battery that, depending on the level of simulation that we want to tackle, can be used (multi-level knowledge model).

To validate the battery pack, the NMC model was incorporated in the simulation of an electric vehicle and compared with the first EMR vehicle model simulated in Simcenter Amesim where the battery was considered a constant ideal voltage source.

The NMC cells present different battery phenomena, detectable in the behavior of the measured battery variables. The model used, captures also:

1. the open circuit voltage that defines the voltage when the battery is at rest.
2. the ohmic resistance, which defines the instantaneous voltage drop, depending on the charge or discharge current.

The equivalent electric circuits for the constant ideal voltage source (from Simcenter Amesim initial library) and NMC models are shown in Figure 47.



Figure 47. Equivalent circuit models: ideal voltage source model (left), NMC model (right)

The two battery models could be expressed, using EMR, as energy source elements (Figure 48). Interaction with the other elements of the BEV system is made through one port, characterized by the power defining variables: battery current i_{bat} and battery voltage u_{bat} (Figure 48). These variables are connected to the power conversion device in the BEV, i.e. chopper, inverter etc. The EMR of the entire BEV is shown in Figure 49, where we can see the physical interaction variables between all the BEV components.

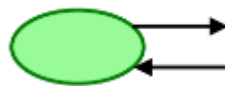


Figure 48. EMR energy source element.

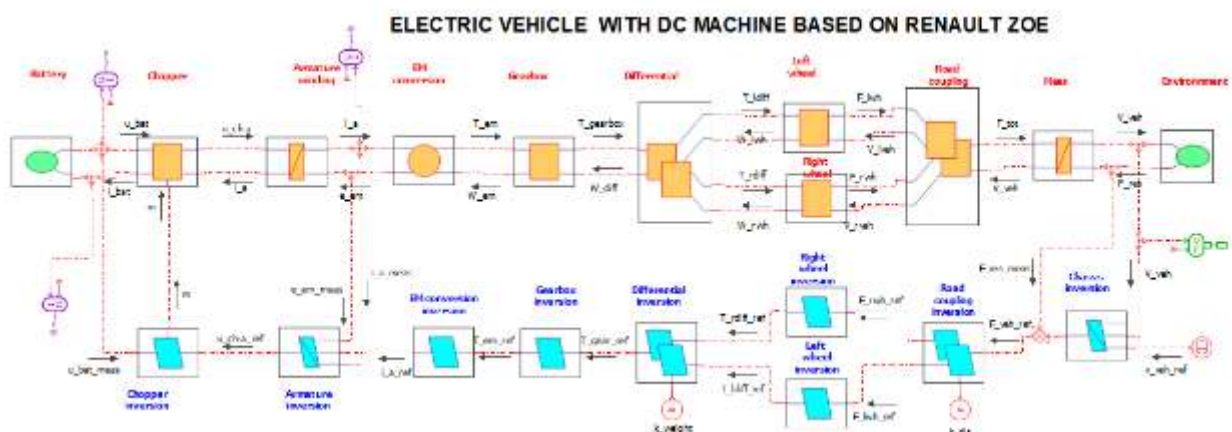


Figure 49. EMR of the BEV.

In addition, the NMC battery model could be represented as a single unit, energy source, or it could be split itself into multiple EMR components, highlighting additional internal power variables (Figure 50).

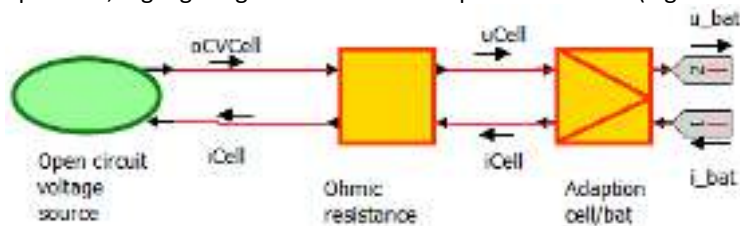


Figure 50. EMR of the NMC battery model.

The battery variables are simulated for the New European Driving Cycle (NEDC) imposed velocity, to show the typical operation of the batteries on an EV driving scenario (Figure 51). By comparing the two models (ideal initial voltage source and quasi-static model proposed in section 4), we see that the more complex model gives more information in the voltage shape, while the current signals are indistinguishable for both models.

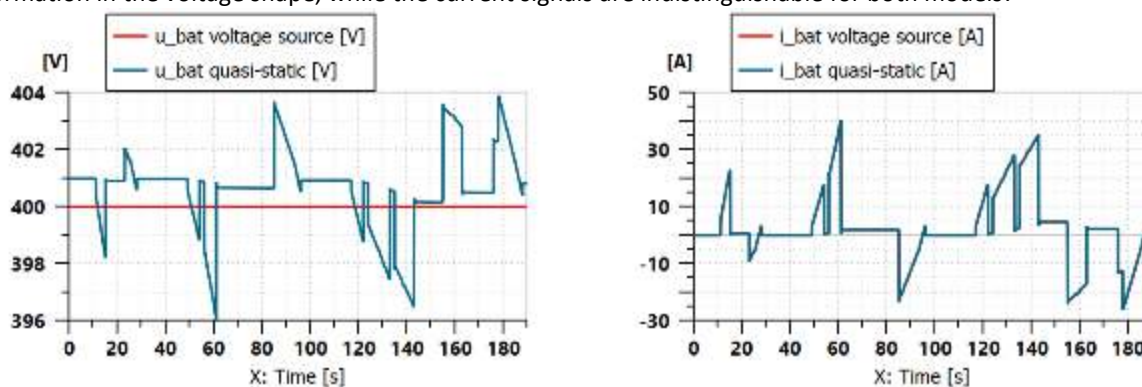


Figure 51. Battery interconnection variables.

The power delivered by the battery is shown in Figure 52, where we notice matching power profiles for both battery models. Even though we saw differences in voltage profiles, the reaction coming from the vehicle in terms of battery current compensates for them. The current differences that compensate for the voltage difference, even if not visible, are present at a smaller scale. The compensating battery current ensures power matching, such that for both models, the same power is delivered in traction, to achieve the same imposed traction performance objectives.

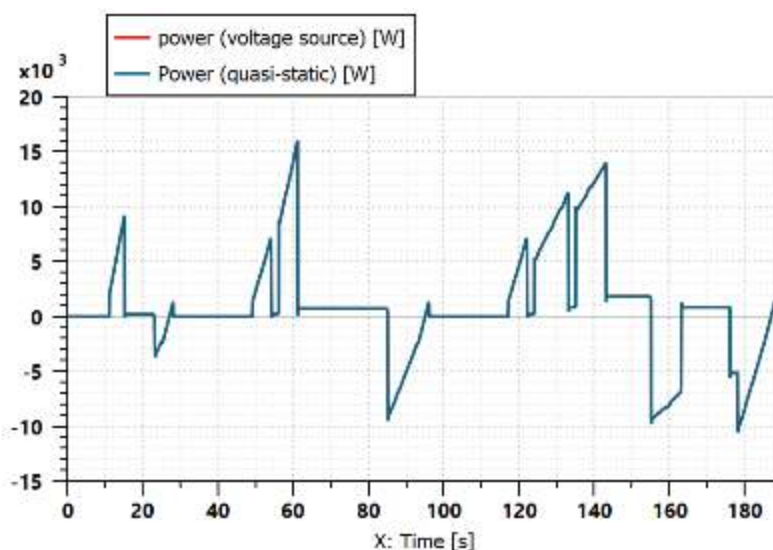


Figure 52. Graph of the battery power.

Because the battery current is provided by the vehicle, given the causal orientation of the current signal, we could attribute the compensating behavior, to achieve power matching, to the control system. The control system calculates the right command such that traction performance criteria are met, in this way influencing the battery current profile.

One of the objectives of the control system is expressed in terms of performance criteria for the armature current control. Figure 53 shows the armature current for both battery models, using the same control system, indicating matching in current tracking performance.

The other objective of the control system is expressed in terms of performance criteria for vehicle velocity tracking. Figure 54 shows the vehicle velocity profiles for both battery modes, indicating matching vehicle velocity performance.

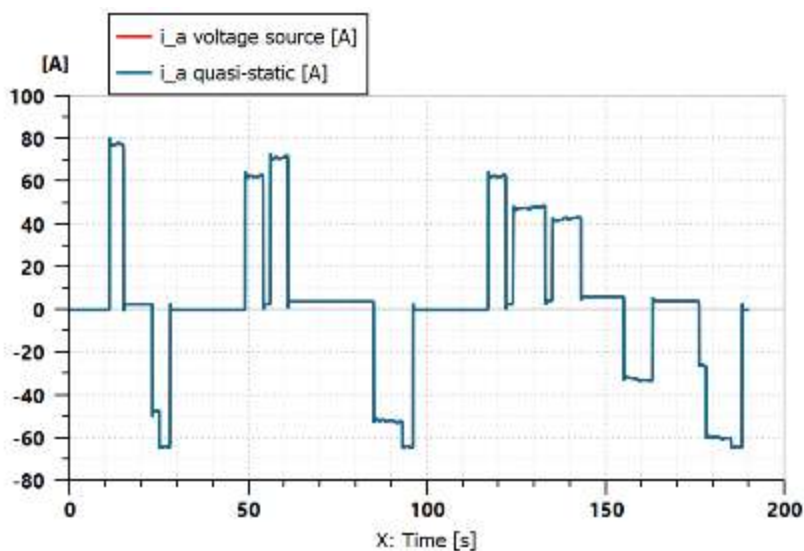


Figure 53. Armature current.

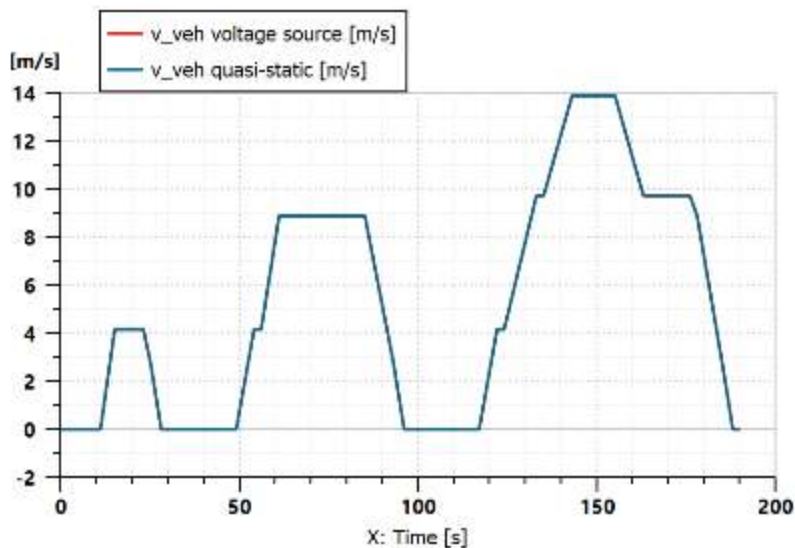


Figure 54. Vehicle velocity

Thus, the armature windings current control system is organized as in the block diagram below.

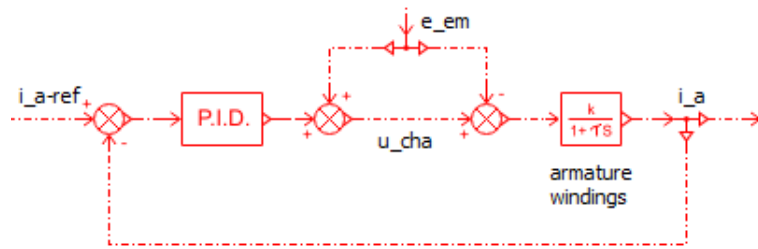


Figure 55. Armature windings current control system.

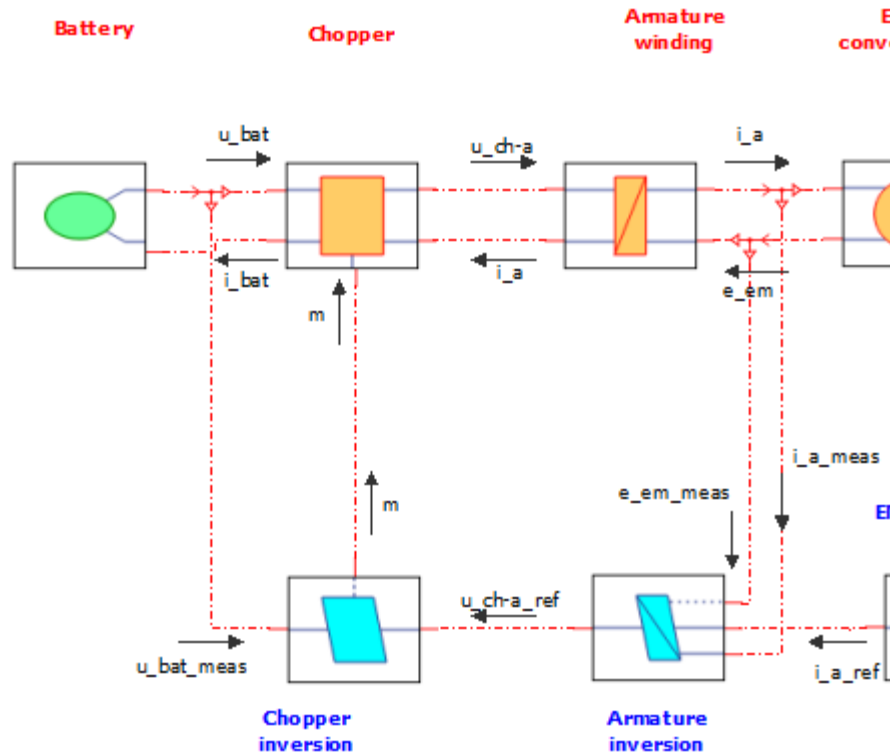


Figure 56. EMR diagram focus on the current control loop.

This block diagram indicates the local nature of the armature windings controller. It also reveals that the traction vehicle performance does not depend on the battery model. The reason is that the interconnection variable i_a does not depend on the battery model. The chopper controller uses the measured battery voltage so that $u_{cha} = u_{cha-ref}$.

Therefore, we can state that: *In the considered EMR configuration, no matter which battery model will be used, it will not influence vehicle traction performance.*

However, we haven't considered unknown disturbances on the battery voltage, which may change the situation, as the relation $u_{cha} = u_{cha-ref}$, would be affected by the disturbance as well.

Even if the battery model is not influencing vehicle performance, still, better battery models help us to better test the energy storage systems. On top of that, the NMC model helps us to simulate the battery state-of-charge, and/or the battery energy management system. We can also use this battery model to reproduce the battery cell variables.

8. Conclusions

The presented report on multi-level modelling provides a detailed model of a battery pack model. The model describes the electro-thermal behavior of a NMC 40 Ah pouch cell and is extended to the pack level. VUB characterization techniques in electro-thermal characterization have allowed in creating a good set of electrical and thermal parameters. They can be implemented in order to perform electric and thermal model activities. The results of the electric-thermal characterization tests highly influence the outcome of the battery model. In this report, electro-thermal characterization tests are performed at different C rates, State of Charge levels and temperatures to include parameters dependence with battery state. Nevertheless the modelling methodology is still valuable for simpler characterizations (constant electro-thermal parameters for example).

The results of the characterization test of the NMC chemistry of the PANDA project were used for the development of a 1D-electro-thermal using the EMR representation for predicting the thermal and the voltage behaviors under static and dynamic load profiles of 40Ah prismatic cells was presented. This model operates on Matlab/Simulink and Simcenter AMESim interface. It is elaborated for a modular approach. From the comparison of both simulations and the experimental results, a good agreement was found with a maximum error of 2 % at cell level and 1% at pack level and 2°C for the electrical and thermal, respectively. Therefore, with the dynamic and static validation profiles performed on this cell, a solid foundation for a generalized model methodology is provided and can be used for WP3 & WP4.

9. Deviations

No deviations with respect to the description of work.

10. References

- [Boulon 2008] T. Huria, M. Ceraolo, J. Gazzarri, and R. Jackey, "High Fidelity Electrical Model with Thermal Dependence for Characterization and Simulation of High Power Lithium Battery Cells," IEEE Int. Electr. Veh. Conf., pp. 1–8, 2012.
- [Bouscayrol 2012] A. Bouscayrol, J. P. Hautier, B. Lemaire-Semail, "Graphic Formalisms for the Control of Multi-Physical Energetic Systems", Systemic Design Methodologies for Electrical Energy, tome 1, Analysis, Synthesis and Management, Chapter 3, ISTE Willey editions, October 2012, ISBN: 9781848213883.
- [Delobel 2017] B. Delobel, I. Jimenez Gordon, and L. Leveau, "ZOE Battery Durability, Field Experience and Future Vision," Adv. Automot. Batter. Conf. Eur., p. 28, 2017.
- [German 2019] B. Delobel, I. Jimenez Gordon, and L. Leveau, "ZOE Battery Durability, Field Experience and Future Vision," Adv. Automot. Batter. Conf. Eur., p. 28, 2017.
- [Goutam 2015] S. Goutam, J. M. Timmermans, N. Omar, P. Van den Bossche, and J. Van Mierlo, "Comparative study of surface temperature behavior of commercial li-ion pouch cells of different chemistries and capacities by infrared thermography," Energies, vol. 8, no. 8, pp. 8175–8192, 2015.
- [Goutam 2016] S. Goutam et al., "Lithium-ion batteries - Analysis of non-uniformity of surface temperature of commercial cells under realistic driving cycles," in EVS 2016 - 29th International Electric Vehicle Symposium, 2016.
- [Hoog 2017] T. Huria, M. Ceraolo, J. Gazzarri, and R. Jackey, "High Fidelity Electrical Model with Thermal Dependence for Characterization and Simulation of High Power Lithium Battery Cells," IEEE Int. Electr. Veh. Conf., pp. 1–8, 2012.
- [Huria 2012] T. Huria, M. Ceraolo, J. Gazzarri, and R. Jackey, "High Fidelity Electrical Model with Thermal Dependence for Characterization and Simulation of High Power Lithium Battery Cells," IEEE Int. Electr. Veh. Conf., pp. 1–8, 2012.
- [Husar 2019] C. Husar, M. Grovu, C. Irimia, A. Desreveaux, A. Bouscayrol, M. Ponchant, P. Magnin, "Comparison of Energetic Macroscopic Representation and structural representation on EV simulation under Simcenter Amesim", IEEE-VPPC'19, Hanoi (Vitenam), October 2019 (Siemens Software and L2EP within the framework of the H2020 PANDA project
- [Incropera 2001] F. P. Incropera and D. P. DeWitt, Fundamentals of Heat and Mass Transfer, Fifth. 2001.
- [Jaguemont 2015] J. Jaguemont, L. Boulon, and Y. Dubé, "A comprehensive review of lithium-ion batteries used in hybrid and electric vehicles at cold temperatures," Appl. Energy, vol. 164, pp. 99–114, 2016.

- [Jaguemont 2016] J. Jaguemont, L. Boulon, P. Venet, and A. Sari, "Lithium Ion Battery Aging Experiments at Sub-Zero Temperatures and Model Development for Capacity Fade Estimation," *IEEE Trans. Veh. Technol.*, vol. PP, no. 99, p. 1, 2015.
- [Omar 2013] N. Omar et al., "Lithium-ion capacitor Advanced technology for rechargeable energy storage systems," *2013 World Electr. Veh. Symp. Exhib.*, vol. 6, pp. 1–11, 2013.
- [Zhang 2011] B. Delobel, I. Jimenez Gordon, and L. Leveau, "ZOE Battery Durability, Field Experience and Future Vision," *Adv. Automot. Batter. Conf. Eur.*, p. 28, 2017.

11. Acknowledgments

The author(s) would like to thank the partners in the project for their valuable comments on previous drafts and for performing the review.

Table 12: Project Partners

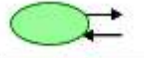
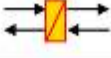
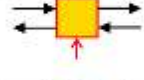
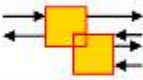
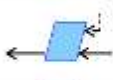
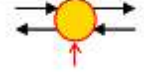
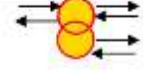
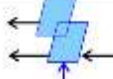
#	Type	Partner	Partner Full Name
1	UNIV	ULille	Université de Lille
2	IND	SISW	Siemens Industry Software SRL
3	UNIV	VUB	Vrije Universiteit Brussels
4	IND	VEEM	VALEO Equipement Electriques Moteur SAS
5	UNIV	UTCN	Universitatea Tehnica Cluj Napoca
6	SME	TY	Tajfun HIL (Typhoon HIL)
7	IND	TUV	TUV SUD AG
8	UNIV	UBFC	Université Bourgogne Franche-Comté
9	SME	UNR	Uniresearch BV
10	IND	RTR	Renault Technologie Roumanie
11	SME	Bluways	BlueWays International bva



This project has received funding from the European Union's Horizon2020 research and innovation programme under Grant Agreement no. 824256.

Appendix A – EMR graphical pictogram

Table 13: EMR pictogram

	Source element (energy source)		Accumulation element (energy storage)		Indirect inversion (closed-loop control)
	Mono-physical conversion element		Mono-physical coupling element (energy distribution)		Direct inversion (open-loop control)
	Multi-physical conversion element		Multi-physical coupling element (energy distribution)		Coupling inversion (energy criteria)

Appendix B – Modelling approach of batteries in Simcenter Amesim

There are three types of battery model in the ESS library as shown in Table 14:

- Simple equivalent circuit model, which consists of a voltage source to represent the open-circuit voltage (OCV) and a resistance. This model would only represent the basic electrical and thermal behaviour of the battery, with few functional parameters and no coupling to other advanced features such as aging and thermal runaway modelling.

- Advanced equivalent circuit model, which in addition can include RC circuits to accurately represent the battery dynamic behaviour related to the diffusion and the charge transfer. This model can be used when is needed to simulate the dynamic behaviour, the aging or the thermal runaway of the battery. Depending on the selected options, the model can have a less complex equivalent circuit. The simplest equivalent circuit corresponds to one of the simple equivalent circuit models. The most complex corresponds to the one shown in Table 14 with RC circuits.

- Electrochemical model, which describes in detail the chemical process taking place inside the battery cell, such as the charge transfer, the diffusion, etc.

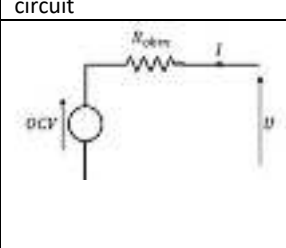
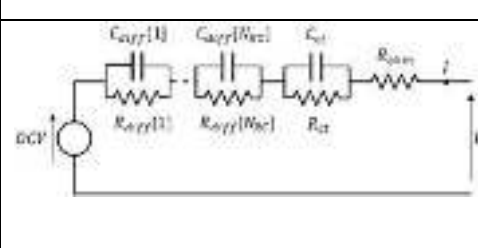
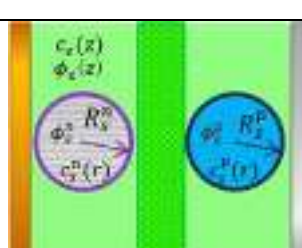
Modelling approach	Simple equivalent circuit	Advanced equivalent circuit	Electrochemical
			
Thermal loss	✓	✓	✓
Thermal runaway	-	✓	-
Aging	-	✓	✓

Table 14. Overview of the battery models.

B1.1 Parameter setting tools

Depending on the state of knowledge of the battery to be modelled, the process of getting the battery cell parameters is very different. Several parameter setting tools are provided in the ESS library to help through these processes:

- Pre-calibrated Tool, which allows generating a battery model corresponding to a commercial cell from a database of commercial cell models which have been tested and validated experimentally.
- Battery Pre-Sizing Tool, which allows generating an ideal battery model that would meet the system requirements by interpolating battery properties in a database of commercial cells.
- Battery Datasheet Import Tool, which allows getting an equivalent circuit model by using the discharge curves in the datasheet of the battery.
- Battery Identification Assistant, which allows identifying an accurate equivalent circuit model from experimental data.
- Transform into RC, which allows transforming the diffusion parameters of a battery.
- BDS Import Tool, which allows importing an equivalent circuit model from a Simcenter BDS (Battery Design Studio) file.

B1.2 Pre-calibrated Tool

The Pre-calibrated Tool allows configuring the battery model by using a database which includes parameter values of different pre-calibrated commercial cells. The workflow of the tool is shown in Figure 57. With the tool, one can choose one of the cells from the database and apply its parameter values to the battery or ultracapacitor model. The resulting model can represent the behaviour of the chosen cell such as the voltage response, the heat flow and the aging.

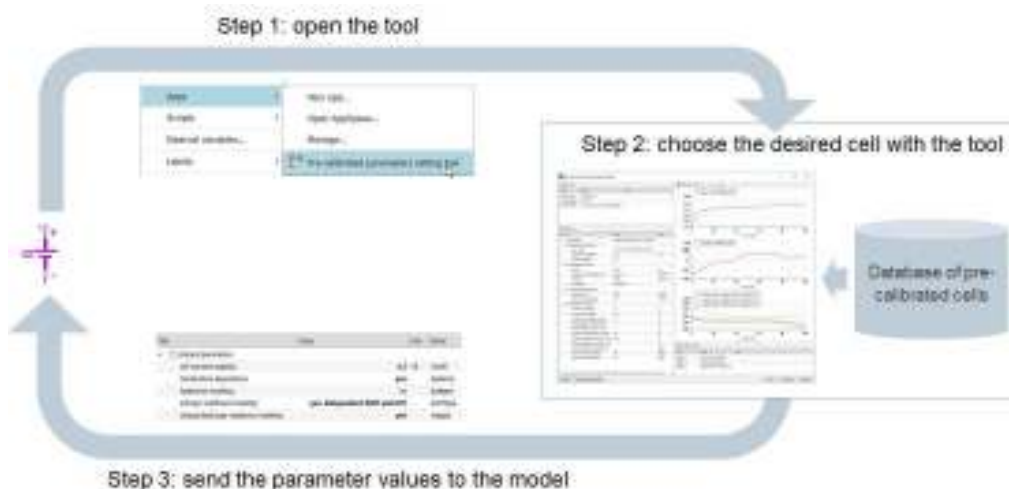


Figure 57. The workflow of the Pre-calibrated Tool.

B1.3 Battery Pre-Sizing Tool

The Battery Pre-Sizing Tool generates parameters for the advanced equivalent circuit cell and pack models according to the technical requirements of the battery pack as shown in Figure 58.

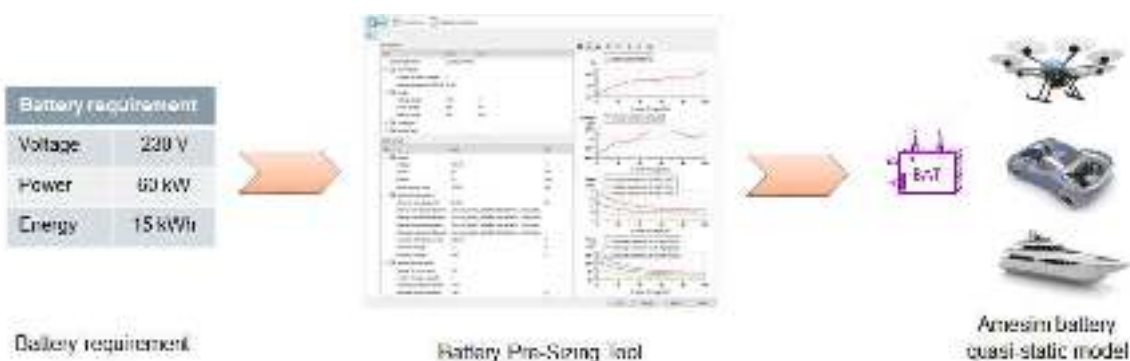


Figure 58. Battery Pre-Sizing Tool objectives.

According to the studies of commercial battery cells, battery properties are similar for two cells of the same chemistry and of the same power/energy (P/E) ratio. Moreover, the values of the properties vary in a predictable way with the P/E ratio. By knowing the P/E ratios and the properties of some reference cells, it is, therefore, possible to interpolate the battery properties for any P/E ratio, as long as it is within the range of the reference cells.

B1.4 Battery Datasheet Import Tool

The Battery Datasheet Import Tool generates parameters for the advanced equivalent circuit cell and pack models. The generated parameters are tables in the function of SOC, but can also include temperature dependence as shown in Figure 59.

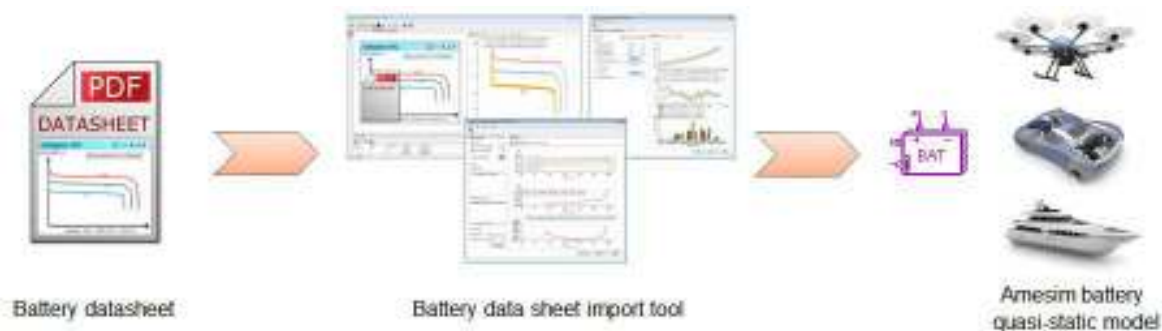


Figure 59. Battery Datasheet Import Tool objectives.

Model parameters can be extracted from the discharge characteristics provided in battery datasheets. The Battery Datasheet Import Tool makes this process straightforward by directly extracting the plot values from datasheet curves. It uses the extracted curves to calculate battery model parameters. It then provides a comparison of the acquired and simulated results, making it easy to judge model fidelity.

Resistance and OCV parameters can be extracted from the datasheet curves. But dynamic battery phenomena, like diffusion, cannot. So the parameterized components will not be able to precisely model the battery's instantaneous voltage. Instead, it is better suited to model the overall electric and thermal energy flow. This makes it perfect for VEM, cooling and other system-level issues.

B1.5 Battery Identification Assistant

The Battery Identification Assistant generates parameters for the advanced equivalent circuit cell and pack models. The generated parameters are tables in the function of SOC and current. Several of these parameters can then be merged together by the Battery Identification Assistant to take temperature dependence into account.



Figure 60. Battery Assistant objectives.

Model parameters can be extracted from test bench measurements of the battery's response to specific current profiles. The identification profile should go over the battery's operating range and measure its response to both positive and negative current pulses. The Battery Identification Assistant can then take these measurements and calculate battery model parameters. It then provides a comparison of the acquired and simulated results, making it easy to judge model fidelity.

From the measurements resistance, O.C.V. and diffusion parameters can be extracted. So the parameterized components will be able to precisely model the battery's instantaneous output voltage. Moreover, by using additional measurements, temperature dependence can be taken into account. This makes the parameterized model perfect for BMS (battery management system) design or other issues where precise modelling of the battery's electrical behaviour is required.

B1.6 Transform into RC

The Transform into RC app makes it easy to switch the diffusion model of an advanced equivalent circuit cell and pack model from resistance and time coefficient (generated by the Battery Identification Assistant) to RC loops.

B1.7 BDS Import Tool

The BDS Import Tool allows importing an equivalent circuit model from a Simcenter BDS (Battery Design Studio) file to the battery advanced equivalent circuit model in Simcenter Amesim. The workflow of the tool is shown in Figure 61.

- Time > 30100 seconds: battery set to 3 consecutive SOC (80%, 50% and 20%) thanks to EV duty cycles and CC discharge at 7.5 A. Then 2 typical road duty cycles are run: the first one is a charge sustaining duty cycle typical of HEV mode and the second one is a charge depleting duty cycle typical of EV mode.

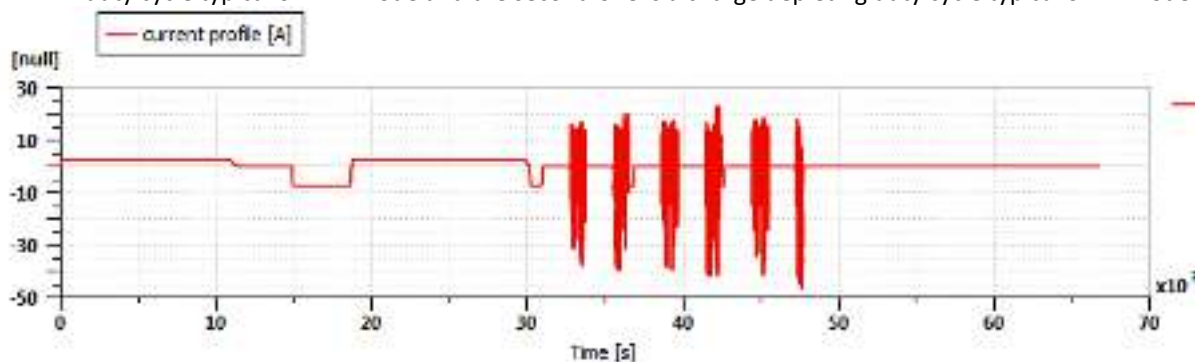


Figure 63. Current profile used for HEV road operation validation.

B.8.2 Model Description

The pre-calibrated NMC model, as shown in Figure 64, has been built and validated using experimental data, provided by IFP Energies Nouvelles test benches [Huria 2012]. The tests were performed on a single prismatic cell. Its nominal capacity is 7.5 Ah as specified by the manufacturer but the measured capacity was 8 Ah. The parameters values of the cell model are saved in the database of the pre-calibrated parameters setting tool. These parameters values can be used by the battery advanced circuit model via the pre-calibrated parameters setting tool.

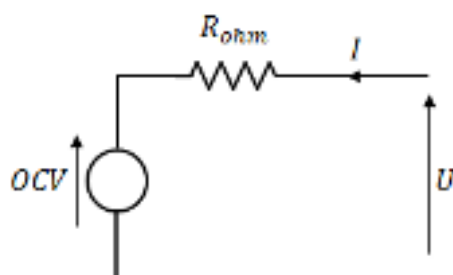


Figure 64. Quasi-static circuit model.

Figure 65 shows the sketch to assess the modelling abilities of the pre-calibrated model. As shown in Figure 18, the cell is linked to a virtual test bench that will provide the current that passed through the cell during actual experimental tests. Experimental data are represented in the measurement from the test bench area.

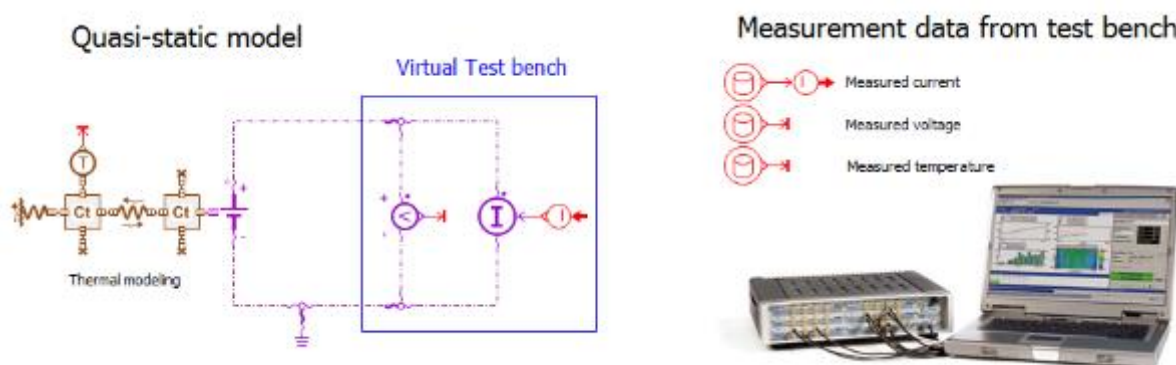


Figure 65. Sketch of the pre-calibrated NMC-CHP model.

B.8.3 Model Parameters

Geometric and thermal parameters of the cells are set according to indications given in the Simcenter AMESsim NMC pre-calibrated cell documentation. The initial SOC is set to 5%. The thermal model consists of 2 masses of

the same thermal capacity representing respectively the core and the skin of the cell. The thermal exchange between the two masses is modelled using a heat conduction coefficient of 0.12 W/m/K and a distance between 2 temperature points of 1 mm for the parameter setting. The environment temperature is set to 39.35 °C and the initial temperature is set to 44 °C according to the experimental measurements. The heat transfer coefficient is set to 30 W/m²/K (fitted against experimental data during the cooling phases).

B.8.4 Analysis

Figure 66 shows a comparison between the experimental data and the model estimation. The voltage simulation results happen to be less accurate during constant current charge than during the duty cycle phase. It is usually the case with quasi-static modeling as slow transient phenomena are not taken into account. The internal resistances are indeed underestimated with low-frequency current inputs. However, the voltage estimation remains very good even during CC phases with a difference between experimental and simulation results lower than 50 mV for SOC higher than 10%. Figure 66 also shows a good agreement between the experimental and the model temperature data during the HEV duty cycle where uncertainty is less than 1 °C. During constant current charge, uncertainty rises as voltage calculations, thus Joule effect, are inaccurate.

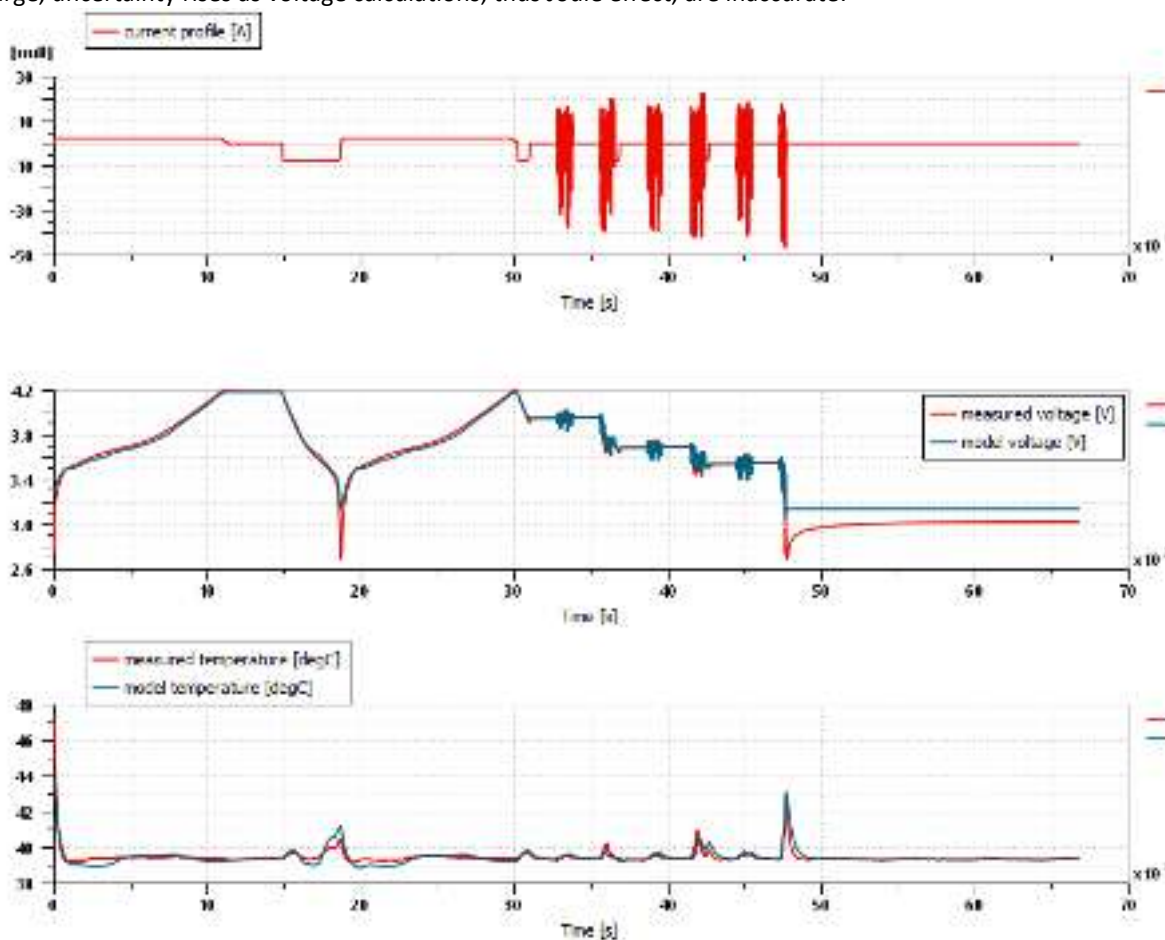


Figure 66. Comparison between experimental voltage and modeling voltages during a typical HEV and EV duty cycles current.

Figure 67 shows the detail of the voltage prediction during an HEV duty cycle (32700 s < t < 33700 s). The simulation voltage is in good agreement with the experimental data during this phase. The electrical and thermal modelling presented in this demo is then validated for typical EV and HEV application usage as well as in CC charges and discharges.

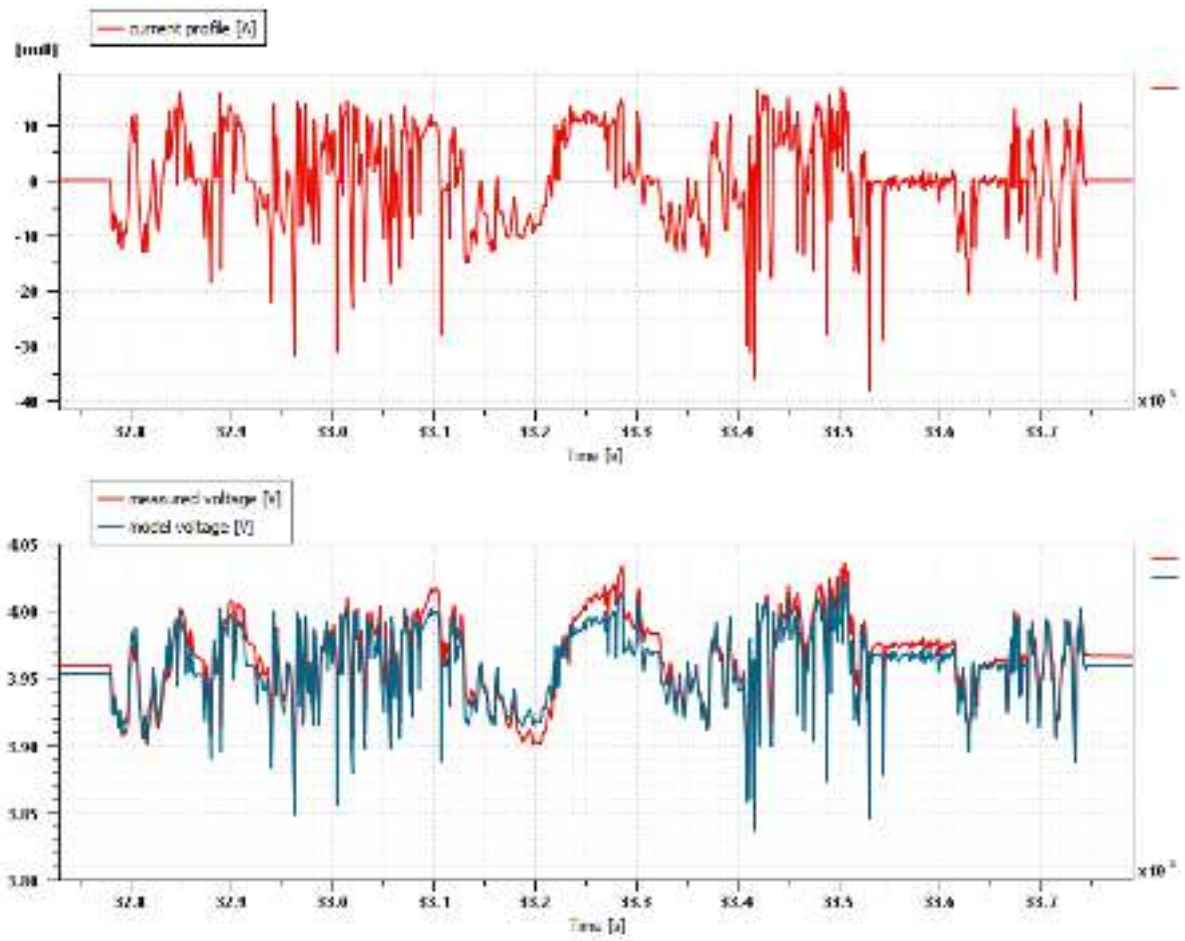


Figure 67. Detailed view of voltage during typical HEV duty cycle.

Appendix C – Quality Assurance

As part of the quality assurance procedure:

- The following questions should be answered by all reviewers (WP Leader, peer reviewer 1, peer reviewer 2 and the technical coordinator);
- Questions answered with NO should be motivated. The author will then make an updated version of the Deliverable. When all reviewers have answered all questions with YES, only then the Deliverable can be submitted to the EC.

NOTE: For public documents, this Quality Assurance part will be removed before publication.

Question	WP Leader	Peer reviewer 1	Peer reviewer 2	Technical Coordinator
	Joris JAGUEMONT	Wim VAN der KUYLEN	Ronan GERMAN	Alain BOUSCAYROL
1. Do you accept this deliverable as it is?	Yes	Yes	Yes	Yes
2. Is the deliverable completely ready? If not, please indicate and motivate required changes.	Yes	Yes	Yes	Yes
3. Does this deliverable correspond to the DoW?	Yes	Yes	Yes	Yes
4. Is the Deliverable in line with the PANDA objectives?	Yes	Yes	Yes	Yes
a. WP Objectives?	Yes	Yes	Yes	Yes
b. Task Objectives?	Yes	Yes	Yes	Yes
5. Is the technical quality sufficient?	Yes	Yes	Yes	Yes